"Double-Locked" and Enzyme-Activated Molecular Probe for Accurate Bioimaging and Hepatopathy Differentiation

Yongchao Liu, Lili Teng, Chengyan Xu, Hong-Wen Liu, Shuai Xu, Haowei Guo, Lin Yuan, Xiao-Bing Zhang*

State Key Laboratory of Chemo/Biosensing and Chemometrics, College of Chemistry and Chemical Engineering, Collaborative Innovation Center for Chemistry and Molecular Medicine, Hunan University, Changsha, 410082. P. R. China.

E-mail: xbzhang@hnu.edu.cn.

Tel: +86-731-88821894

Table of contents

1. Experimental details

Reagents and Apparatus. All chemicals were purchased from commercial suppliers and used without further purification. MitoTracker Green, LysoTracker Green, ERTracker Red and radioimmuno precipitation assay (RIPA) lysis buffer were purchased from Beyotime Biotechnology. Leucine aminopeptidase (LAP), monoamine oxidase A (MAO) were purchased from Sigma-Aldrich. The commercial kits (ALT, AST, MAO) were purchased from Nanjing Jiancheng Bioengineering Institute, LAP commercial kit was purchased from Qiyi Biotechnology (Shanghai) Co., Ltd. All the enzymes (LAP, MAO, GGT, Tyr) were dissolved into pure water to form aqueous solution and were divided into several parts for daily experiments. To maintain the enzyme activity, all these solutions were stored at -80 °C before using. The mice were purchased from Hunan Slake Jingda Laboratory Animal Co., Ltd. Water was purified and doubly distilled by a Milli-Q system (Millipore, USA). The UV-Visible absorption spectra were acquired *via* Shimadzu UV-2600 UV-VIS-NIR spectrophotometer. Fluorescence spectra were recorded on a HITACHI F4600 fluorescence spectrophotometer with a 1 cm standard quartz cell. Mass spectra were performed using an LCQ Advantage ion trap mass spectrometer (Thermo Finnigan). NMR spectra were recorded on a Bruker DRX-400 spectrometer using TMS as an internal standard. Thin layer chromatography (TLC) was conducted using silica gel 60 F254 and column chromatography was carried out over silica gel (200-300 mesh), which were obtained from Qingdao Ocean Chemicals (Qingdao, China). The pH was measured with a Mettler-Toledo Delta 320 pH meter. Fluorescence images of cells were obtained from Olympus FV1000-MPE laser scanning confocal-microscope (Japan). The fluorescent images of mice and serum were obtained *via* an IVIS Lumina XR Imaging System (Caliper, U.S.A.) equipped with a cooled charge coupled device (CCD) camera. Circular ROIs were drawn over the areas and quantified by Lumina XR Living Image software, version 4.3. The serum sample from healthy people (three), hepatitis b patients (three), and cirrhotic patients (three) were kindly supplied by the First Hospital of Changsha City.

Spectral Measurements. The fluorescence measurement experiments were performed in PBS (10 mM) with DMSO as co-solvent solution (PBS/DMSO = 9:1, v/v, 10 mM, pH = 7.4). For the probe respond to LAP or MAO, a volume of 20 μL of **NM**, **NL** or **NML** stock solution (0.1 mM), 0-20 μL of LAP solution (1000 U/L), 0-20 μL of MAO solution (1000 U/L), and PBS buffer solution were added into a tube to make the final volume 200 μL. The reaction solution was transferred into a quartz cell to measure the absorbance or fluorescence spectra, with both excitation and emission slits set at 5 nm. Different pH values of PBS solution from 4.0 to 9.0 were adjusted by adding minimal volumes of HCl solution or NaOH solution. The solutions of various testing species were prepared

preliminary by using double-distilled water with the final interference concentration. The fluorescence spectra were measured with excitation wavelength at 670 nm.

Cell Culture and Imaging. HepG2 cells were maintained in RPMI-1640 medium with 10% fetal bovine serum (FBS, GIBCO) and 1% penicillin-streptomycin at 37 °C in a humidified atmosphere containing 20% O_2 and 5% CO_2. When the cell density reached 90% of confluence, a subculture was performed and the medium was changed approximately every day. Cells were seeded in a 20 mm glass-bottom dish plated and grown to around 80% confluency for 24 h before the experiment. Fluorescence imaging of cells was carried out using an Olympus FV1000 MPE laser scanning microscope (Japan) with a 60× oil immersion objective lens. The fluorescence signal of cells incubated with **NML** was collected in the channel (650-750 nm) by using a semiconductor laser at 635 nm as the excitation source. The fluorescent images of mice and serum were obtained via an IVIS Lumina XR Imaging System (Caliper, U.S.A.) equipped with a cooled charge coupled device (CCD) camera with the collected channel (Cy 5.5: λ_{ex} = 640 nm, λ_{em} = 695−770 nm). Circular ROIs were drawn over the areas and quantified by Lumina XR Living Image software, version 4.3.

Cytotoxicity Assay. Cytotoxicity assays were carried out using HepG2 cells. Cell viability was determined using the CCK-8 assay. 5000 cells per well were seeded in a 96-well plate and incubated for 12 h in a humidified incubator for adherence. **NML** were dissolved in DMSO, and the solution was then added to cells at the final concentration of 0, 2, 4, 6, 8, 10, 15, 20 μM and incubated for 24 h. CCK-8 reagent diluted by RPMI-1640 (FBS free) medium (10%) was added to each well after the removal of culture media and incubated for 0.5 h. Following that, the absorbance was measured at 450 nm on a plate reader Synergy 2 Multi-Mode Microplate Reader (Bio-Tek, Winooski, VT).

HepG2 Tumor Model. All animal procedures were performed in accordance with the Guidelines for Care and Use of Laboratory Animals of Hunan University and experiments were approved by the Animal Ethics Committee of College of Biology (Hunan University). About 10^6 HepG2 cells were grafted into a nude BALB/C mouse. Tumors with diameters of around 10 mm were formed after 20 and 30 days, respectively.

Fluorescence imaging of acetaminophen (APAP) induced liver injury in BALB/c. 30 female BALB/c (18-20 g) mice were divided into 6 groups on average; group 1: intraperitoneal injected PBS + intravenous injection **NML**, group 2: intraperitoneal injected APAP + intravenous injection **NML**, group 3: intraperitoneal injected with PBS + intravenous injected with **NM**, group 4: intraperitoneal injected with APAP + intravenous injected with **NM**, group 5: intraperitoneal injected with PBS + intravenous injected with **NL**, group 6: intraperitoneal injected with APAP + intravenous injected with **NL**. Mice were intraperitoneal injected with 100 μL of 200 mg/kg

acetaminophen (APAP) or 100 μL PBS for 1h, then intravenous injected with 50 μL of 100 μM **NM**, **NL**, or **NML** for 40 min, 80 min and 120 min. Subsequently, the mice were immediately imaged *via* an IVIS Lumina XR Imaging System. Circular ROIs were drawn over each well, and fluorescent intensity was quantified by Living Image software.

Construction of acetaminophen (APAP) induced liver injury (DILI) models in KM mice. 25 female KM (18-20 g) mice were divided into 5 groups on average; group 1: APAP 0 h (control), group 2: APAP 3 h, group 3: APAP 6 h, group 4: APAP 9 h, group 5: APAP 12 h. Mice were intraperitoneal injected with 200 μL of 200 mg/kg acetaminophen (APAP). For the control group, the mice were administered an intraperitoneal injection of PBS buffer (200 μL). Then, the mice were sacrificed after different administration times, then the blood and liver tissues were collected. The liver tissues were excised for histological examination by standard H&E staining. The blood was left at room temperature for 30 min and centrifuged for 10 minutes under 3000 rpm to take serum. The serum was stored in a -80°C refrigerator before testing. In both methods, serum samples were 10-fold diluted for *in vitro* measurement.

Construction of tetrachloromethane (CCl_4) induced liver cirrhosis models in KM mice. 42 female KM (18-20 g) mice were divided into 6 groups on average; group 1: CCl_4-0 day (control), group 2: CCl_4-8 days, group 3: CCl_4-16 days, group 4: CCl_4-24 days, group 5: CCl_4-32 days, group 6: CCl_4-40 days. Mice were subcutaneously injected with 50 μL 40% concentration of CCl_4 diluted with cotton seed oil for 40 days. In the meantime, the mice were maintained with 30% ethanol in water as drinking water. The mice were sacrificed after different administration days, then the blood was collected. The liver tissues were excised for histological examination by standard H&E staining. The blood was left at room temperature for 30 min and centrifuged for 10 minutes under 3000 rpm to take serum. The serum was stored in a -80°C refrigerator before testing. In both methods, serum samples were 10-fold diluted for *in vitro* measurement.

General Procedure for *in vitro* serum testing. The samples were 10-fold diluted for *in vitro* measurement. Briefly, a volume of 10 μL of **NML**, **NM**, or **NL** stock solution (200 μM), 10 μL diluted serum, PBS buffer solution (180 μL) were added into the wells of 96-well flat-bottom black plate to make the final volume 200 μL, and then incubated with at 37 °C for 2 h (for **NL**, the incubated time is 30 min). Subsequently, the black plate was immediately measured *via* an IVIS Lumina XR Imaging System. Circular ROIs were drawn over each well, and fluorescent intensity was quantified by Living Image software.

Procedure for Determining LAP with Commercial Assay Kit. In this kit, the detection mechanism of LAP is based on LAP hydrolysis of L-leucyl p-nitroaniline to p-nitroaniline, which has a maximum absorption peak at 405

nm, and the LAP activity is calculated by measuring the rate of increase in absorbance at 405 nm. In brief, 50 μL of the serum samples were added to a quartz cuvette, and the final volumes of the samples were adjusted to 200 μL with the LAP assay buffer containing L-leucyl p-nitroaniline. Immediately after mixing, record the initial absorbance at 405 nm (A1) and absorbance (A2) were recorded after 2 min and calculated as ΔA = A2-A1. Finally, LAP activity was calculated based on the given equation in the manufacturer's instructions: LAP (nmol/min/mL) = $[\Delta A \times V_1 \div (\varepsilon \times d) \times 10^9] \div V_2 \div T = 205.8 \times \Delta A$. V_1: the total volume of the reaction system (200 μL), V_2: the volume of serum (50 μL), ε: molar extinction coefficient of p-nitroaniline (9.72×10^3 L/mol/cm), d: the diameter of the cuvette (1 cm), T: reaction time (2 min).

Procedure for Determining MAO with Commercial Assay Kit. In this kit, the mechanism of MAO activity determination is based on MAO catalyzed deamination of monoamine substrate to form corresponding aldehyde, which is further oxidized to acid. The substrate has a characteristic absorption peak at 242 nm, and the MAO activity is calculated by measuring the rate of increase in absorbance at 242 nm. In brief, 20 μL of the serum samples were added to a quartz cuvette, then added MAO assay regent 1 (300 μL) and 2 (3 mL), followed by incubation at 37 °C for 3 h and then added assay regent 3 (300 μL) and 4 (3 mL), mixed and centrifuged for 10 minutes (3500 rpm), absorbance (A) at 242 nm was recorded. Finally, the MAO activity was calculated based on the given equation following the manufacturer's instructions: MAO (nmol/h/mL) = $(A-A_0)/0.01/T/V=1666.7 \times \Delta A$. A: absorbance of serum sample at 242 nm, A_0: absorbance of water sample at 242 nm, T: reaction time (3 h), V: the volume of serum (20 μL).

2. Compound Synthesis

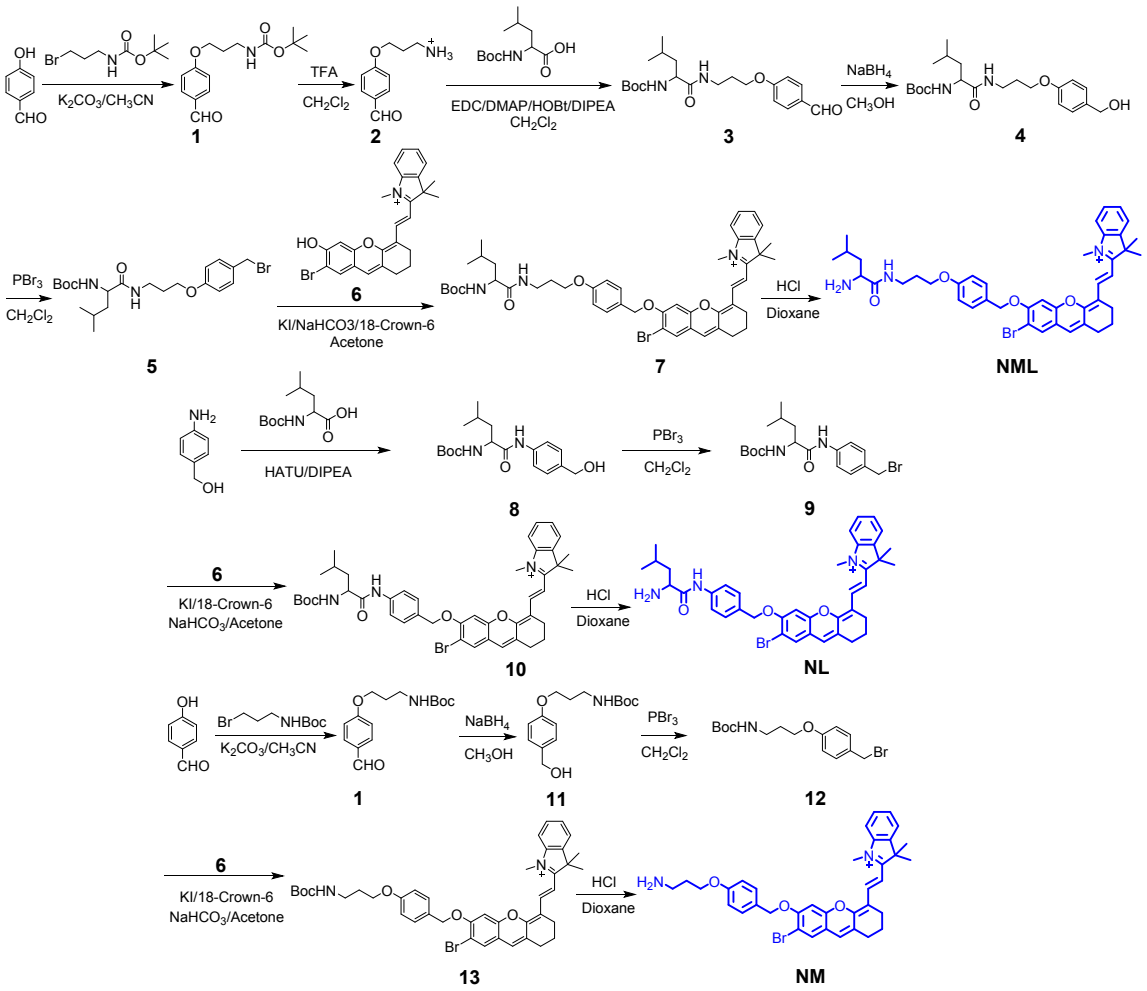

Scheme S1 Synthetic route of **NML**, **NL** and **NM**.

Synthesis of Compound 1. *p*-hydroxy benzaldehyde (2.44 g, 20 mmol), tert-butyl (3-bromopropyl) carbamate (5.95 g, 25 mmol) and anhydrous potassium carbonate (13.8 g, 100 mmol) were placed in a flask containing CH_3CN (80 mL), and the mixture was stirred at 85 °C for 10 h. The solution was cooled and separated by filtration. The filtrate was removed under reduced pressure and the product was obtained as colorless oily liquid (4.81 g, yield 86 %) without purification. ^{1}H NMR (400 MHz, $CDCl_3$) δ 9.79 (s, 1H), 7.74 (d, J = 8.0 Hz, 2H), 6.92 (d, J = 8.1 Hz, 2H), 5.07 (s, 1H), 4.04 (t, J = 5.5 Hz, 2H), 3.27 (s, 2H), 1.95 (d, J = 7.1 Hz, 2H), 1.37 (s, 9H). ^{13}C NMR (101 MHz, $CDCl_3$) δ 190.73, 163.85, 156.06, 131.90, 129.85, 114.70, 79.07, 66.00, 37.60, 29.46, 28.34.

Synthesis of Compound 2. Compound 1 (2.79 g, 10 mmol) was dissolved in TFA/CH_2Cl_2 (20 mL/20 mL) at room temperature for 30 min. The solvent was removed by evaporation under reduced pressure, and the obtained crude product 2 was directly used in the following reaction without further purification.

Synthesis of Compound 3. Compound 2 (1.79 g, 10 mmol), (tert-butoxycarbonyl) leucine (2.31 g, 10 mmol),

EDCI (1.55 g, 10 mmol), DMAP (1.22 g, 10 mmol), HOBt (1.35 g, 10 mmol), DIPEA (3.87 g, 30 mmol) were dissolved in CH_2Cl_2 (50 mL) at room temperature for 10 h. Then the solution was washed with water and brine, dried with anhydrous Na_2SO_4. The solvent was removed under reduced pressure and the residue was purified by flash chromatography column using petroleum ether/ ethyl acetate (2/1) as eluent to give compound 3 as a white solid (2.45 g, yield 62.5 %). ^{1}H NMR (400 MHz, $CDCl_3$) δ 9.87 (s, 1H), 7.82 (d, *J* = 8.1 Hz, 2H), 7.00 (d, *J* = 8.1 Hz, 2H), 6.73 (s, 1H), 5.05 (d, *J* = 6.4 Hz, 1H), 4.10 (t, *J* = 5.4 Hz, 3H), 3.46 (d, *J* = 3.6 Hz, 2H), 2.08-2.00 (m, 2H), 1.66 (d, *J* = 5.7 Hz, 2H), 1.54-1.46 (m, 1H), 1.43 (d, *J* = 7.8 Hz, 9H), 0.93 (s, 6H). ^{13}C NMR (101 MHz, $CDCl_3$) δ 190.80, 172.89, 163.74, 155.84, 131.99, 130.02, 114.74, 80.09, 66.21, 53.22, 41.23, 36.74, 28.98, 28.29, 24.77, 22.93, 21.96.

Synthesis of Compound 4. To a suspension of compound 3 (1.18 g, 3.0 mmol) in CH_3OH (80 mL) at 0 °C, $NaBH_4$ (228 mg, 6 mmol) was added slowly. After 30 min, the resulting suspension was stirred for 2 h at room temperature. Then the mixture was diluted with dichloromethane (100 mL), and washed with water and brine. The organic layer was separated and dried over anhydrous Na_2SO_4. The solvent was removed by evaporation under reduced pressure, and the residue was subjected to silica gel chromatography with petroleum ether/ ethyl acetate (1/1) as eluent, obtaining compound 4 as a white solid (1.00 g, yield 85%). ^{1}H NMR (400 MHz, DMSO) δ 7.89 (s, 1H), 7.21 (d, *J* = 7.5 Hz, 2H), 6.86 (d, *J* = 7.4 Hz, 3H), 5.05 (s, 1H), 4.41 (d, *J* = 4.4 Hz, 2H), 3.94 (s, 3H), 3.36 (s, 2H), 3.20 (s, 2H), 1.83 (s, 2H), 1.56 (s, 1H), 1.37 (s, 9H), 0.89-0.81 (m, 6H). ^{13}C NMR (101 MHz, DMSO) δ 173.00, 157.89, 155.77, 134.96, 128.32, 114.47, 78.35, 65.65, 63.01, 53.31, 41.35, 35.98, 29.32, 28.64, 24.76, 23.36, 22.09.

Synthesis of Compound 5. To a solution of compound 4 (985 mg, 2.5 mmol) in CH_2Cl_2 (50 mL) at 0 °C, tribromophosphine (0.474 mL, 5.0 mmol) was added dropwise. The resulting reaction mixture was warmed up to room temperature and stirred for 5 h. Then, the mixture was diluted with dichloromethane (20 mL), and washed with water and brine. The organic layer was separated and dried with anhydrous Na_2SO_4. The solvent was removed by evaporation under reduced pressure, and the obtained crude product 5 was directly used in the following reaction without further purification.

Synthesis of Compound 6. 4-Bromoresorcinol (1.88 g, 10 mmol) and Et_3N (2 mL) were placed in a flask containing DMF (10 mL), and the mixture was stirred at 50 ℃ under nitrogen atmosphere for 10 min. Compound 1 (3.0 g, 5 mmol) in DMF (10.0 mL) was introduced to the mixture via a syringe, and the reaction mixture was heated at 55 °C for 6 h. Then, the reaction solution was poured into ice water and extracted with CH_2Cl_2. The combined organic solution was concentrated under reduced pressure. After purified by the silica gel

chromatography (CH_2Cl_2/EtOH, 10:1, v/v), compound 6 was obtained as a blue-green solid (2.24g, 38%). ^{1}H NMR ($CDCl_3$, 400 MHz) δ 8.14 (d, *J* = 8.11 Hz, 1H), 7.59 (s, 1H), 7.32-7.29 (m, *J* = 7.30 Hz, 3H), 7.10-7.06 (t, *J* = 7.08Hz, 1H), 6.87 (d, *J* = 6.86 Hz, 1H), 6.70 (s, 1H), 5.62 (d, *J* = 5.61 Hz, 1H), 3.37 (s, 3H), 2.70-2.67 (t, *J* = 2.69 Hz, 2H), 2.64-2.61 (t, *J* = 2.62 Hz, 2H), 1.86 (t, *J* = 1.90 Hz, 2H), 1.63 (s, 6 H).

Synthesis of Compound 7. Compound 6 (462 mg, 1 mmol), compound 5 (912 mg, 2 mmol), $NaHCO_3$ (168 mg, 2 mmol), 18-crown-6 (264 mg, 1 mmol) and KI (1.66 g, 10 mmol) were mixed in 40 mL acetone, and the resulting mixture was stirred at 40 ºC under nitrogen for 24 h. Then, dichloromethane (50 mL) was added, and the resulting solution was washed water and brine, dried with anhydrous Na_2SO_4. After removal of the solvent, the residue was purified by flash chromatography on silica gel using CH_2Cl_2/CH_3OH (200/1~50/1) as eluent to afford the compound 7 as a blue-violet solid (246.7 mg, yield 29%). ^{1}H NMR (400 MHz, $CDCl_3$) δ 8.60 (d, *J* = 14.9 Hz, 1H), 7.56 (d, *J* = 9.8 Hz, 2H), 7.47 (d, *J* = 7.6 Hz, 3H), 7.45-7.40 (m, 2H), 7.11 (s, 1H), 7.03 (s, 1H), 6.92 (d, *J* = 7.7 Hz, 2H), 6.86 (d, *J* = 8.0 Hz, 1H), 6.78 (d, *J* = 11.8 Hz, 1H), 6.50 (d, *J* = 14.9 Hz, 1H), 5.31 (s, 2H), 5.06 (d, *J* = 7.0 Hz, 1H), 4.07 (s, 3H), 4.02 (d, *J* = 5.6 Hz, 2H), 3.44 (s, 2H), 2.73 (d, *J* = 18.7 Hz, 4H), 2.28 (d, *J* = 7.0 Hz, 2H), 2.00 (d, *J* = 6.1 Hz, 2H), 1.90 (s, 2H), 1.82 (s, 6H), 1.65 (d, *J* = 4.0 Hz, 2H), 1.45 (s, 3H), 1.42 (s, 9H), 0.92 (d, *J* = 4.4 Hz, 6H). ^{13}C NMR (101 MHz, $CDCl_3$) δ 178.11, 172.82, 160.71, 158.73, 157.66, 153.35, 145.82, 142.13, 141.59, 131.53, 130.83, 129.33, 129.12, 128.56, 127.64 (s, 4H), 122.60, 116.48, 115.25, 114.53, 112.86, 109.45, 105.15, 101.57, 77.32, 71.78, 66.18, 53.51, 50.90, 37.09, 34.87, 29.27, 29.02, 28.06, 24.77, 23.02, 21.93, 20.16.

Synthesis of NML. To a solution of compound 7 (100 mg, 0.12 mmol) in CH_2Cl_2 (2 mL) at 0 °C, a dioxane - hydrochloride solution (1 mL, 4 mol/L) was added dropwise, and the resulting mixture was stirred at 0 ºC under nitrogen for 10 min. Then the residue was quickly purified by flash chromatography on silica gel using CH_2Cl_2/CH_3OH (100/1) as eluent to afford the **NML** as a blue-violet solid (30 mg, yield 41%). ^{1}H NMR (400 MHz, MeOD) δ 8.71 (d, *J* = 14.9 Hz, 1H), 7.70 (d, *J* = 6.8 Hz, 2H), 7.59 (dd, *J* = 16.3, 7.5 Hz, 2H), 7.48 (dd, *J* = 13.8, 7.5 Hz, 3H), 7.22 (d, *J* = 9.9 Hz, 2H), 6.98 (d, *J* = 7.6 Hz, 2H), 6.56 (d, *J* = 15.0 Hz, 1H), 5.28 (s, 2H), 4.04 (d, *J* = 5.2 Hz, 2H), 3.91 (s, 3H), 3.82 (s, 1H), 3.67 (s, 1H), 2.82-2.67 (m, 4H), 2.05-1.99 (m, 2H), 1.92 (s, 2H), 1.84 (s, 6H), 1.65 (d, *J* = 6.0 Hz, 3H), 1.28 (s, 2H), 0.98-0.92 (m, 6H). ^{13}C NMR (101 MHz, MeOD) δ 178.08, 172.79, 160.68, 158.70, 157.63, 153.32, 145.80, 142.10, 141.56, 131.51, 130.80, 129.30, 129.10, 128.53, 127.62, 122.57, 116.46, 115.23, 114.50, 112.84, 109.42, 105.13, 101.55, 71.75, 66.16, 53.49, 50.87, 37.06, 34.85, 29.24, 28.99, 28.03, 24.74, 22.99, 21.91, 20.13. ESI-MS: m/z calcd for **NML** ($C_{42}H_{49}BrN_3O_4^+$, [M]), 740.29; found, 740.2.

Synthesis of Compound 8. Boc-L-Leucine (1.16 g, 5 mmol) was dissolved in DCM (100 mL), followed by

addition of HATU (2.28 g, 6 mmol) and DIPEA (1.65 mL, 10 mmol). After further stirring over 30 min, (4-aminophenyl) methanol (1.23 g, 10 mmol) was added, and then the mixture reacted for 12 h at room temperature. The resultant was washed with water and brine. The organic layer was separated and dried with anhydrous Na_2SO_4. The crude product was purified by silica-gel column chromatography using dichloromethane/methanol (50:1) to afford compound 8 (1.14 g, 68% yield). ^{1}H NMR (400 MHz, DMSO) δ = 9.89 (s, 1H), 7.56 (d, *J*=6.9, 2H), 7.25 (d, *J*=6.8, 2H), 6.98 (d, *J*=5.7, 1H), 5.10 (s, 1H), 4.45 (s, 2H), 4.14 (s, 1H), 2.69 (s, 2H), 1.54 (s, 1H), 1.39 (s, 9H), 0.90 (s, 6H). ^{13}C NMR (101 MHz, DMSO) δ = 172.06, 155.89, 138.10, 137.82, 127.33, 119.47, 78.46, 63.08, 54.08, 53.98, 41.22, 28.64, 23.41, 22.03.

Synthesis of Compound 9. To a solution of compound 8 (840 mg, 2.5 mmol) in CH_2Cl_2 (50 mL) at 0 °C, tribromophosphine (0.474 mL, 5.0 mmol) was added dropwise. The resulting reaction mixture was warmed up to room temperature and stirred for 5 h. Then, the mixture was diluted with dichloromethane (20 mL), and washed with water and brine. The organic layer was separated and dried with anhydrous Na_2SO_4. The solvent was removed by evaporation under reduced pressure, and the obtained crude product 9 was directly used in the following reaction without further purification.

Synthesis of NL. Compound 6 (462 mg, 1 mmol), compound 9 (798 mg, 2 mmol), $NaHCO_3$ (168 mg, 2 mmol), 18-crown-6 (264 mg, 1 mmol) and KI (1.66 g, 10 mmol) were mixed in 40 mL acetone, and the resulting mixture was stirred at 40 ºC under nitrogen for 24 h. Then, dichloromethane (50 mL) was added, and the resulting solution was washed water and brine, dried with anhydrous Na_2SO_4. After removal of the solvent, the residue was purified by flash chromatography on silica gel using CH_2Cl_2/CH_3OH (200/1~50/1) as eluent to afford the compound 10 as a blue-violet solid. To a solution of compound 10 (100 mg, 0.13 mmol) in CH_2Cl_2 (2 mL) at 0 °C, a dioxane - hydrochloride solution (1 mL, 4 mol/L) was added dropwise, and the resulting mixture was stirred at 0 ºC under nitrogen for 10 min. Then the residue was quickly purified by flash chromatography on silica gel using CH_2Cl_2/CH_3OH (100/1) as eluent to afford the **NL** as a blue-violet solid (23 mg, yield 26%). ^{1}H NMR (400 MHz, MeOD) δ = 8.71 (d, *J* = 15.1, 1H), 7.72 (dd, *J* = 7.1, 4H), 7.60 (d, *J* = 7.4, 1H), 7.57 (d, *J* = 8.1, 1H), 7.56 – 7.52 (m, 2H), 7.50 (dd, *J* = 10.4, 1H), 7.21 (d, *J* = 14.7, 2H), 6.56 (d, *J* = 15.1, 1H), 5.34 (s, 2H), 4.58 (s, 2H), 3.98 (t, *J* = 6.4, 1H), 3.90 (s, 3H), 3.65 (s, 1H), 2.73 (dt, *J* = 12.1, 4H), 1.96-1.87 (m, 2H), 1.84 (d, *J* = 3.0, 6H), 1.76 (d, *J* = 6.5, 2H), 1.28 (s, 1H), 1.01 (dd, *J* = 5.7, 6H). ^{13}C NMR (101 MHz, MeOD) δ = 178.88, 169.09, 160.32, 157.46, 153.29, 145.75, 142.26, 137.88, 132.25, 131.07, 130.87, 128.83, 128.43, 127.88, 127.39, 124.88, 122.33, 120.02, 116.71, 114.49, 112.68, 108.56, 104.75, 101.18, 70.93, 52.65, 50.83, 41.03, 31.73, 29.34, 28.78, 26.69, 24.21, 23.65, 21.87, 20.82, 20.14. ESI-MS: m/z calcd for **NL** ($C_{39}H_{43}BrN_3O_3^+$, [M]), 682.25; found, 682.06.

Synthesis of Compound 11. To a suspension of compound 1 (837 mg, 3.0 mmol) in CH_3OH (80 mL) at 0 °C, $NaBH_4$ (228 mg, 6 mmol) was added slowly. After 30 min, the resulting suspension was stirred for 2 h at room temperature. Then the mixture was diluted with dichloromethane (100 mL), and washed with water and brine. The organic layer was separated and dried over anhydrous Na_2SO_4. The solvent was removed by evaporation under reduced pressure, and the residue was subjected to silica gel chromatography with petroleum ether/ ethyl acetate (1/1) as eluent, obtaining compound 11 as a white solid (741 mg, yield 88%). ^{1}H NMR (400 MHz, DMSO) δ = 7.21 (d, *J* = 8.6, 2H), 6.86 (d, *J* = 8.6, 2H), 5.02 (s, 1H), 3.94 (t, *J* = 6.3, 2H), 3.07 (dd, *J* = 12.8, 6.7, 2H), 1.81 (p, *J* = 6.6, 2H), 1.37 (s, 9H). ^{13}C NMR (101 MHz, DMSO) δ = 157.93, 156.10, 134.95, 128.33, 114.48, 77.95, 65.69, 63.02, 37.44, 29.73, 28.71.

Synthesis of Compound 12. To a solution of compound 11 (702 mg, 2.5 mmol) in CH_2Cl_2 (50 mL) at 0 °C, tribromophosphine (0.474 mL, 5.0 mmol) was added dropwise. The resulting reaction mixture was warmed up to room temperature and stirred for 5 h. Then, the mixture was diluted with dichloromethane (20 mL), and washed with water and brine. The organic layer was separated and dried with anhydrous Na_2SO_4. The solvent was removed by evaporation under reduced pressure, and the obtained crude product 12 was directly used in the following reaction without further purification.

Synthesis of Compound 13. Compound 6 (462 mg, 1 mmol), compound 12 (688 mg, 2 mmol), $NaHCO_3$ (168 mg, 2 mmol), 18-crown-6 (264 mg, 1 mmol) and KI (1.66 g, 10 mmol) were mixed in 40 mL acetone, and the resulting mixture was stirred at 40 ºC under nitrogen for 24 h. Then, dichloromethane (50 mL) was added, and the resulting solution was washed water and brine, dried with anhydrous Na_2SO_4. After removal of the solvent, the residue was purified by flash chromatography on silica gel using CH_2Cl_2/CH_3OH (200/1~50/1) as eluent to afford the compound 13 as a blue-violet solid. ^{1}H NMR (400 MHz, MeOD) δ = 8.67 (d, *J* = 14.9, 1H), 7.68 (d, *J* = 8.1, 2H), 7.57 (t, *J* = 8.7, 2H), 7.49 (d, *J* = 7.1, 1H), 7.44 (d, *J* = 7.8, 2H), 7.24 (d, *J* = 7.5, 1H), 7.19 (s, 1H), 7.14 (s, 1H), 6.94 (d, *J* = 7.6, 2H), 6.87 (d, *J* = 7.4, 1H), 6.53 (d, *J* = 15.0, 1H), 5.26 (s, 2H), 3.99 (d, *J* = 4.1, 2H), 3.89 (s, 3H), 3.21 (s, 2H), 2.76-2.67 (m, 4H), 1.94-1.89 (m, 4H), 1.83 (s, 6H), 1.40 (s, 9H). ^{13}C NMR (101 MHz, MeOD) δ = 178.79, 160.36, 159.12, 157.58, 153.27, 145.69, 142.27, 142.16, 131.17, 130.81, 128.81, 128.74, 128.30, 128.20, 127.88, 127.36, 122.29, 116.60, 114.46, 114.34, 114.02, 112.64, 108.69, 104.68, 101.23, 78.55, 71.22, 65.34, 50.82, 37.06, 31.84, 29.37, 28.78, 27.37, 26.85, 26.74, 23.71, 20.13.

Synthesis of NM. To a solution of compound 13 (100 mg, 0.14 mmol) in CH_2Cl_2 (2 mL) at 0 °C, a dioxane - hydrochloride solution (1 mL, 4 mol/L) was added dropwise, and the resulting mixture was stirred at 0 ºC under nitrogen for 10 min. Then the residue was quickly purified by flash chromatography on silica gel using

CH_2Cl_2/CH_3OH (100/1) as eluent to afford the **NM** as a blue-violet solid (32 mg, yield 36.5 %). ^1H NMR (400 MHz, MeOD) δ = 8.73 (d, *J* = 15.1, 1H), 7.75-7.68 (m, 2H), 7.61 (d, *J* = 7.6, 1H), 7.58-7.53 (m, 1H), 7.52-7.46 (m, 3H), 7.24 (d, *J* =12.6, 2H), 7.03 (d, *J* = 8.7, 2H), 6.57 (d, *J* = 15.1, 1H), 5.30 (s, 2H), 4.15 (t, *J* = 5.8, 2H), 3.92 (s, 3H), 3.17 (t, *J* = 7.3, 2H), 2.80-2.69 (m, 4H), 2.20-2.14 (m, 2H), 1.99-1.88 (m, 2H), 1.85 (s, 6H). ^{13}C NMR (101 MHz, MeOD) δ = 178.87, 160.31, 158.68, 157.56, 145.70, 142.27, 142.20, 131.10, 130.83, 128.96, 128.81, 128.38, 127.36, 122.30, 116.64, 114.49, 114.37, 112.70, 104.79, 101.19, 71.11, 64.96, 50.82, 37.55, 37.23, 31.83, 28.80, 26.96, 26.67, 23.70, 20.16. ESI-MS: m/z calcd for **NM** ($C_{36}H_{38}BrN_2O_3^+$, [M]), 625.21; found, 625.07.

3. Optical properties and biological studies

Probe	NML	NM	NL	NF
λ_{abs}/nm[a]	605	604	602	694
λ_{em}/nm[b]	687	690	688	720
Φ_f [c]	< 0.01	< 0.01	< 0.01	0.152

Table S1 Quantum yield, absorption and emission wavelengths of NML, NM, NL, NF. a. The maximal absorption of the dye. b. The maximal emission of the dyes. c. Φ_f is the relative fluorescence quantum yield estimated by using indocyanine green (ICG, Φ_f = 0.13 in DMSO).

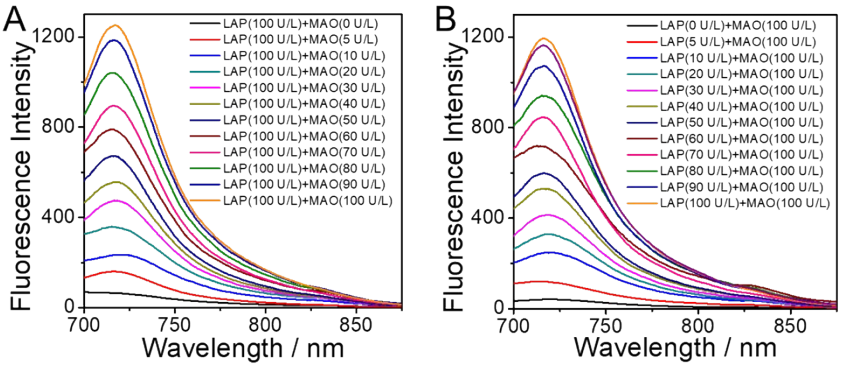

Fig. S1 (A) Emission spectra of **NML** (10 μM) with LAP (100 U/L) and different concentrations of MAO (0-100 U/L). (B) Emission spectra of **NML** (10 μM) with MAO (100 U/L) and different concentrations of LAP (0-100 U/L). λ_{ex} = 670 nm.

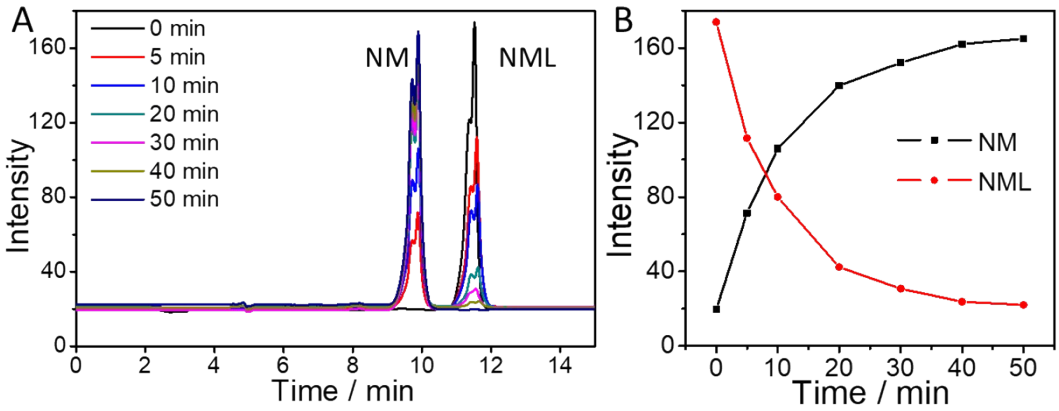

Fig. S2 (A) Chromatograms of **NML** (50 μM) treated with **LAP** (1000 U/L) for different times. (B) The kinetics of LAP reacting with **NML**. The quantitative intensity and retention time were recorded from (A). Retention time: t(NM) = 9.987 min, t(NML) = 11.676 min. Detection: UV-vis (600 nm) detector. Flow rate: 1 mL/min. T: 25 °C. Injection volume: 200 μL. Mobile phase: acetonitrile/water = 70/30 (v/v) for 10 min, then acetonitrile/water = 70/30 (v/v) for 10 min.

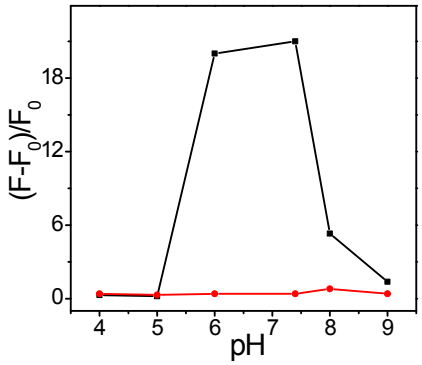

Fig. S3 Effects of pH on the fluorescence intensity of **NML** (10 μM) with (black curve) or without (red curve) LAP (100 U/L) and MAO (100 U/L). The measurements were performed at 37 °C in PBS buffer solution with $\lambda_{ex/em}$ = 670/720 nm.

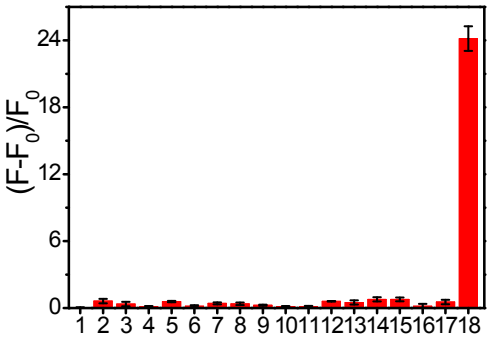

Fig. S4 Fluorescence response $(F-F_0)/F_0$ of **NML** (10 μM) in the presence of diverse ions in buffer solution (pH 7.4) at 37 °C. (1) blank; (2) KCl (15 mM); (3) $CaCl_2$ (2.5 mM); (4) $MgCl_2$ (2.5 mM); (5) H_2S (100 μM); (6) glucose (10 mM); (7) vitamin C (1 mM); (8) GSH (1 mM); (9) Cys (1 mM), (10) Arg (1 mM); (11) Ala (1 mM);

(12) ClO^- (100 μM); (13) H_2O_2 (100 μM); (14) GGT (100 U/L); (15) Tyr (200 U/L); (16) LAP (100 U/L); (17) MAO (100 U/L); (18) LAP (100 U/L) + MAO (100 U/L). $\lambda_{ex/em}$ = 670/720 nm. The results are the mean standard deviation of three separate measurements.

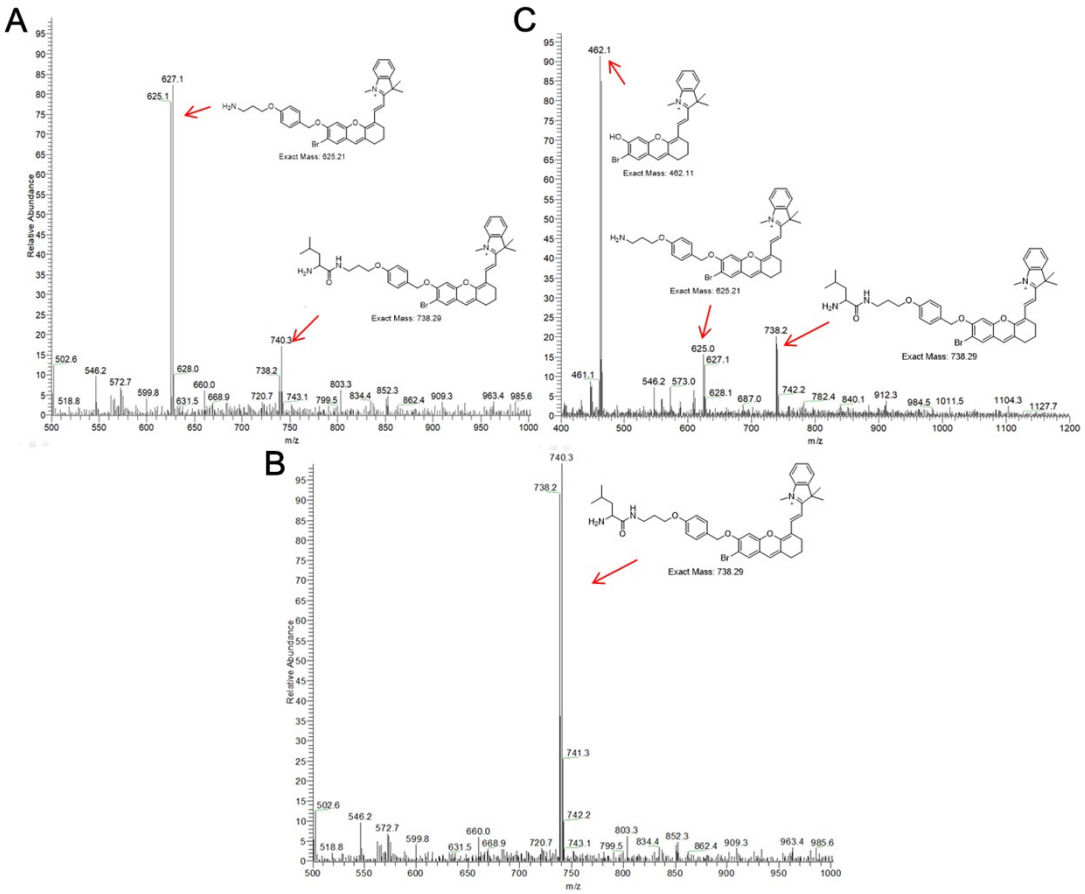

Fig. S5 ESI mass spectra of the reaction solutions of **NML** with (A) LAP (B) MAO (C) LAP and MAO.

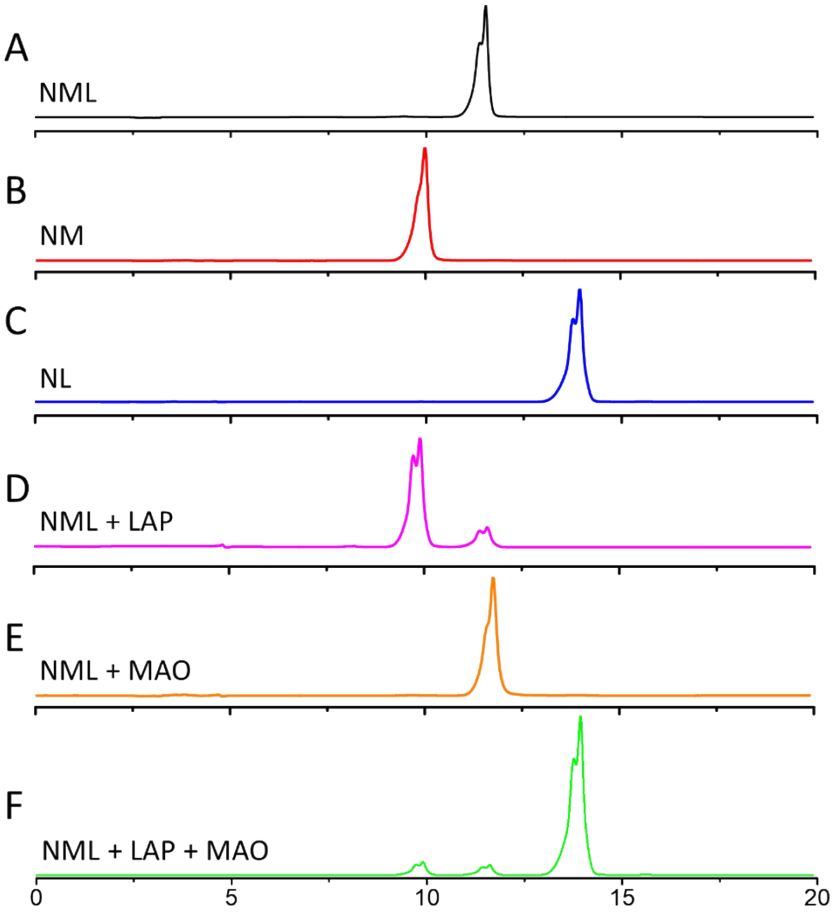

Fig. S6 Chromatograms of different reaction systems. (A) 50 μM **NML**; (B) 50 μM **NM**; (C) 50 μM **NL**; (D) the reaction products of 50 μM **NML** treated with 1000 U/L LAP for 30 min; (E) the reaction products of 50 μM **NML** treated with 1000 U/L MAO for 2 h; (F) the reaction products of 50 μM **NML** treated with 1000 U/L LAP and 1000 U/L MAO for 2 h; Retention time: t(NM) = 9.987 min, t(NML) = 11.676 min, t(NF) = 13.929 min,. Detection: UV-vis (600 nm) detector. Flow rate: 1mL/min. T: 25 °C. Injection volume: 200 μL. Mobile phase: acetonitrile/water = 70/30 (v/v) for 10 min, then acetonitrile/water = 70/30 (v/v) for 10 min.

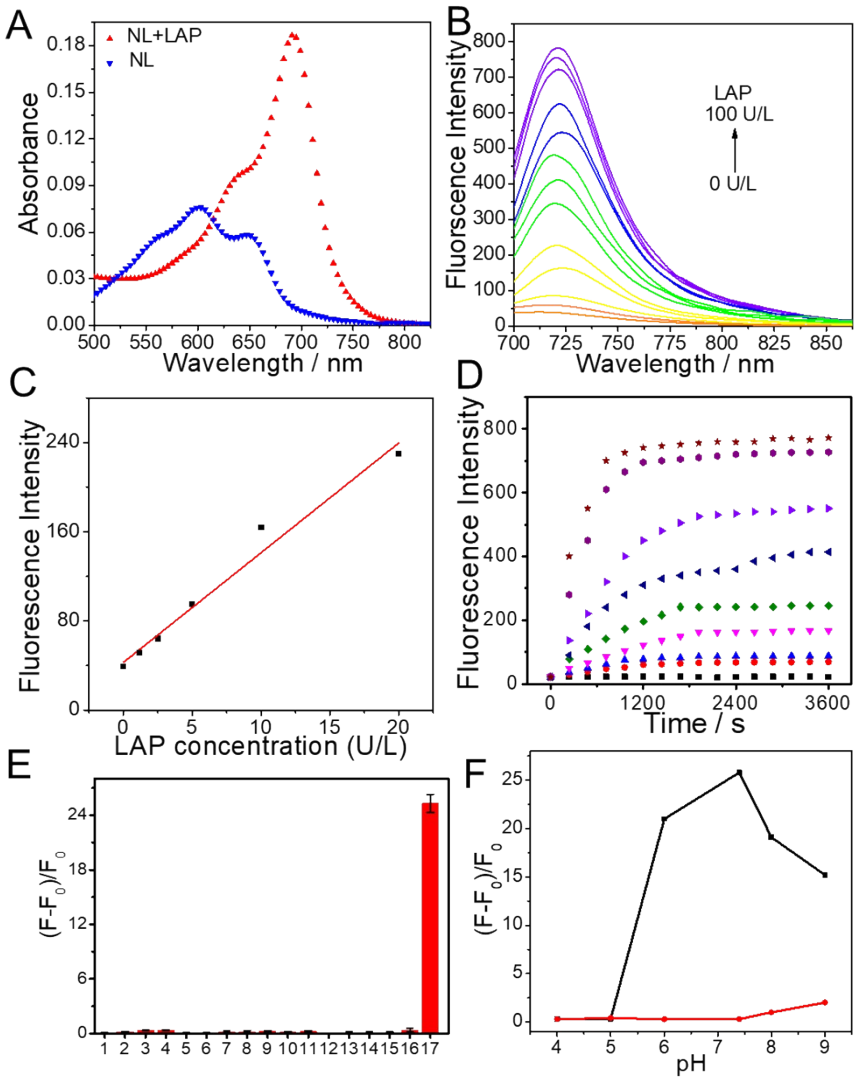

Fig. S7 Fluorescence properties of **NL** and its response to LAP. (A) Normalized absorption spectra of **NL** (10 μM) before and after reaction with LAP (100 U/L). (B) Emission spectra of **NL** (10 μM) at different concentrations of LAP. Insert picture: Emission spectra at low concentrations of LAP. (C) Linear fluorescence responses at low concentrations of LAP. (D) Time-dependent response of **NL** (10 μM) to LAP with different concentrations (0, 2, 5, 10, 20, 40, 60, 80, 100 U/L). (E) Fluorescence response $(F-F_0)/F_0$ of **NL** (10 μM) in the presence of diverse ions in buffer solution (pH 7.4) at 37 °C. (1) blank; (2) KCl (15 mM); (3) $CaCl_2$ (2.5 mM); (4) $MgCl_2$ (2.5 mM); (5) H_2S (100 μM); (6) glucose (10 mM); (7) vitamin C (1 mM); (8) GSH (1 mM); (9) Cys (1 mM), (10) Arg (1 mM); (11) Ala (1 mM); (12) ClO^- (100 μM); (13) H_2O_2 (100 μM); (14) GGT (100 U/L); (15) Tyr (200 U/L); (16) MAO (100 U/L); (17) LAP (100 U/L). $\lambda_{ex/em}$ = 670/720 nm. The results are the mean standard deviation of three separate measurements. (F) Effects of pH on the fluorescence intensity of **NL** (10 μM) with (black curve) or without (red curve) LAP (100 U/L). $\lambda_{ex/em}$ = 670/720 nm.

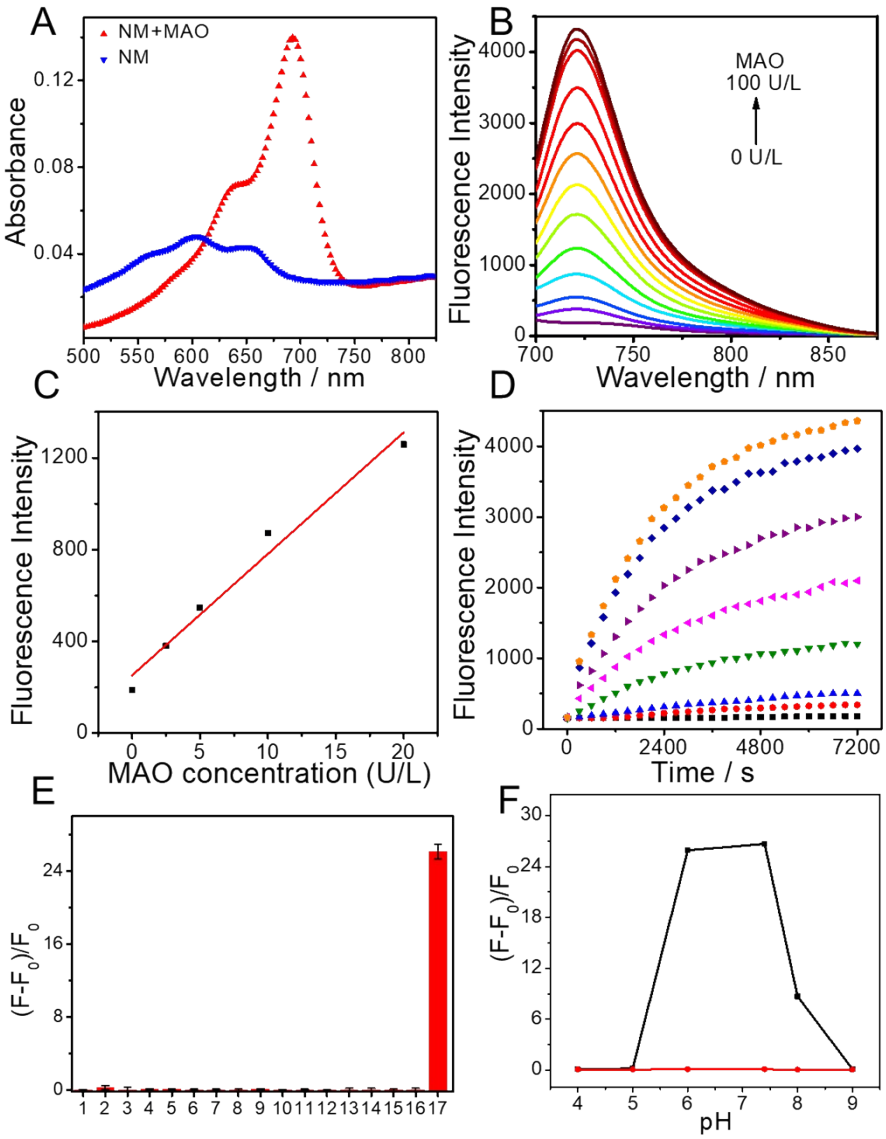

Fig. S8 Fluorescence properties of **NM** and its response to MAO. (A) Normalized absorption spectra of **NM** (10 μM) before and after reaction with MAO (100 U/L). (B) Emission spectra of **NM** (10 μM) at different concentrations of MAO. (C) Linear fluorescence responses at low concentrations of MAO. (D) Time-dependent response of **NM** (10 μM) to MAO with different concentrations (0, 2.5, 5, 20, 40, 60, 80, 100 U/L). (E) Fluorescence response $(F-F_0)/F_0$ of **NM** (10 μM) in the presence of diverse ions in buffer solution (pH 7.4) at 37 °C. (1) blank; (2) KCl (15 mM); (3) $CaCl_2$ (2.5 mM); (4) $MgCl_2$ (2.5 mM); (5) H_2S (100 μM); (6) glucose (10 mM); (7) vitamin C (1 mM); (8) GSH (1 mM); (9) Cys (1 mM), (10) Arg (1 mM); (11) Ala (1 mM); (12) ClO^- (100 μM); (13) H_2O_2 (100 μM); (14) GGT (100 U/L); (15) Tyr (200 U/L); (16) LAP (100 U/L); (17) MAO (100 U/L). $\lambda_{ex/em}$ = 670/720 nm. The results are the mean standard deviation of three separate measurements. (F) Effects of pH on the fluorescence intensity of **NM** (10 μM) with (black curve) or without (red curve) MAO (100 U/L). $\lambda_{ex/em}$ = 670/720 nm.

Detection limit	Enzyme	NML	NM	NL
	LAP (U/L)	0.25[a]	——	0.11
	MAO (U/L)	0.12[b]	0.028	——

Table S2. The detection limit (3σ/slope) of NML, NM and NL. a. The detection limit is measured under the condition that the MAO concentration is 100 U/L. b. The detection limit is measured under the condition that the LAP concentration is 100 U/L.

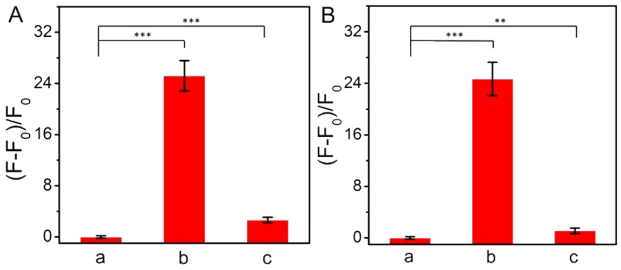

Fig. S9 (A) Fluorescence response $(F-F_0)/F_0$ of **NL** (10 μM) in different reaction systems: a: **NL**, b: **NL** + LAP; c: **NL** + LAP + Bestatin. (B) Fluorescence response $(F-F_0)/F_0$ of **NM** (10 μM) in different reaction systems: a: **NM**; b: **NM** + MAO; c: **NM** + MAO + Clorgiline; LAP: 100 U/L, MAO: 100 U/L, Bestatin: 100 μM, Clorgiline: 10 nM. The measurements were performed at 37 °C in PBS (pH 7.4) with $\lambda_{ex/em}$ = 670/720 nm. The results are the mean standard deviation of three separate measurements. $^{**}P < 0.01$, $^{***}P < 0.001$, compared with the control group (normal group).

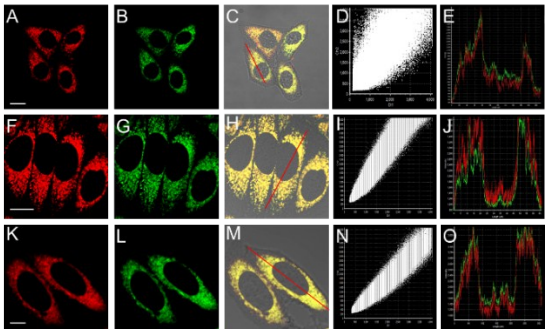

Fig. S10 Colocalization experiments in HepG2 cells. Fluorescence image of cells incubated with (A-E) **NML** (10 μM) for 2 h; (F-J) **NM** (10 μM) for 2 h; (K-O) **NL** (10 μM) for 30 min and then MitoTracker Green (100 nM) for 30 min. (A, F, K) Red channel: λ_{ex}= 635 nm, λ_{em}= 650-750 nm; (B, G, L) Green channel: λ_{ex} = 488 nm, λ_{em} = 500-600 nm. Scale bar: 20 μm. (C, H, M) Merged image of red channel and green channel. (D, I, N) Colocalization scatterplots of (C, H, M), respectively. (D) PC: 0.925; (I) PC: 0.957; (N) PC: 0.928. (E, J, O) Intensity profile of regions of interest that marked by the red line in (C, H, M).

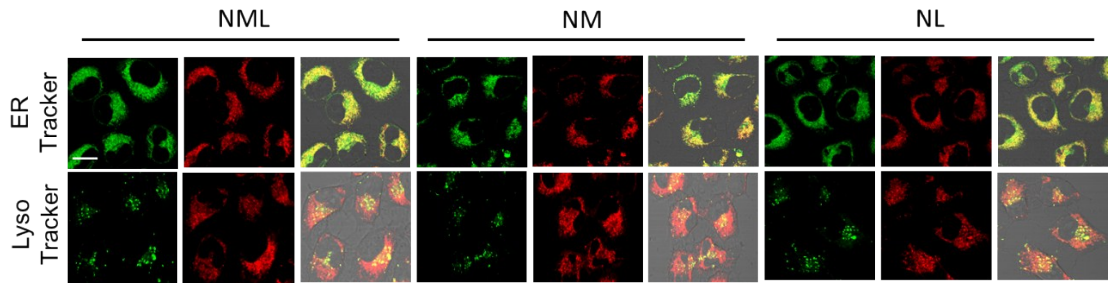

Fig. S11 Colocalization experiments of **NML**, **NM**, **NL** with ERTracker Red and LysoTracker Green in HepG2 cells. Fluorescence image of cells incubated with **NML** (10 μM) for 2 h; **NM** (10 μM) for 2 h; (a-e) **NL** (10 μM) for 30 min and then ERTracker Red (100 nM) or LysoTracker Green (100 nM) for 30 min. ERTracker Red: λ_{ex}= 559 nm, λ_{em}= 580-620 nm; LysoTracker Green: λ_{ex} = 488 nm, λ_{em} = 500-600 nm; **NML**, **NM**, **NL**: λ_{ex}= 635 nm, λ_{em}= 650-750 nm. Scale bar: 20 μm.

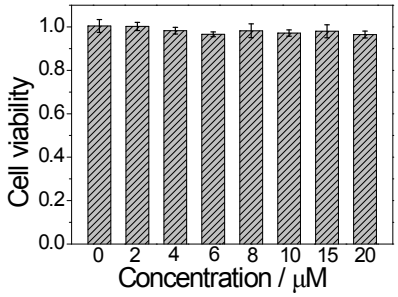

Fig. S12 Cell viability of HepG2 cells treated with different concentrations of **NML** for 24 h in fresh medium. The results are the mean standard deviation of five separate measurements.

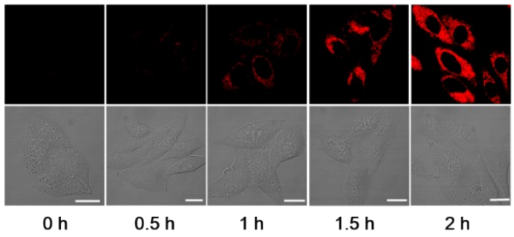

Fig. S13 Fluorescence images of HepG2 cells incubated with **NML** (10 μM) for different periods of time (0, 0.5, 1, 1.5 and 2 h). DIC images of the corresponding samples are shown in the second row. λ_{ex}= 635 nm, λ_{em}= 650-750 nm. Scale bar: 20 μm.

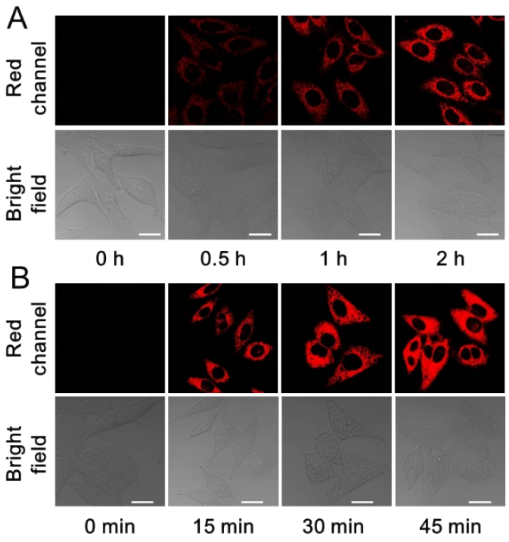

Fig. S14 Fluorescence images of HepG2 cells incubated with (A) **NM** (10 μM) for different periods of time (0, 0.5, 1 and 2 h), (B) **NL** (10 μM) for different periods of time (0, 15, 30 and 45 min). DIC images of the corresponding samples are shown in the bottom row. λ_{ex}= 635 nm, λ_{em}= 650-750 nm. Scale bar: 20 μm.

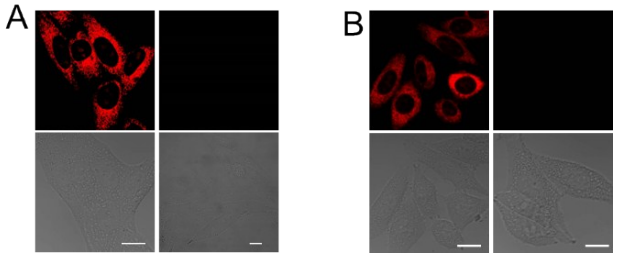

Fig. S15 Fluorescence images of HepG2 cells incubated with **NL** (10 μM) or **NM** (10 μM) for different treatments: (a) left line: **NL**; right line: **NL** + Bestatin (100 μM), (b) left line: **NM**; right line: **NM** + Clorgiline (10 nM). λ_{ex}= 635 nm, λ_{em}= 650-750 nm. Scale bar: 20 μm.

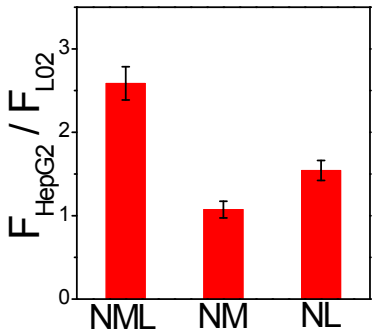

Fig. S16 Fluorescence intensity ratio (F_{HepG2}/F_{L02}) of **NML**, **NM** or **NL** in HepG2 and L02 cells lysis buffer. Cells were washed with DPBS three times, then removal of the DPBS, a radioimmuno precipitation assay (RIPA) lysis buffer was added into the culture dish to obtain protein lysates. Protein concentrations were measured with protein detector. The results are the mean standard deviation of three separate measurements.

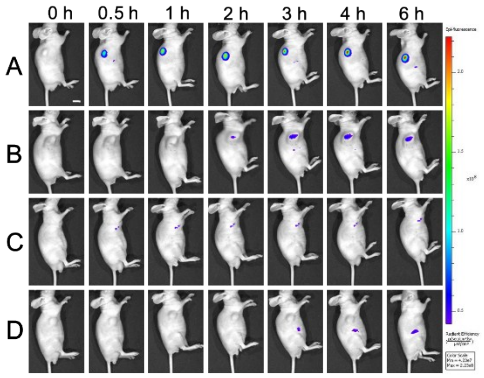

Fig. S17 *In vivo* fluorescence imaging of HepG2 tumor xenografted mice. The mice were intratumorally preinjected with 50 μL of (A) PBS (control), (B) Bestatin: 100 μM, (C) Clorgiline: 100 nM, (D) Bestatin: 100 μM + Clorgiline: 100 nM for 1 h, and then subjected to intratumoral injection of 50 μL **NML** (50 μM) in PBS for different periods of time (0, 0.5, 1, 2, 3, 4 and 6 h). Scale bar: 1 cm. Ex= 640 nm. The emission band was at 695-770 nm.

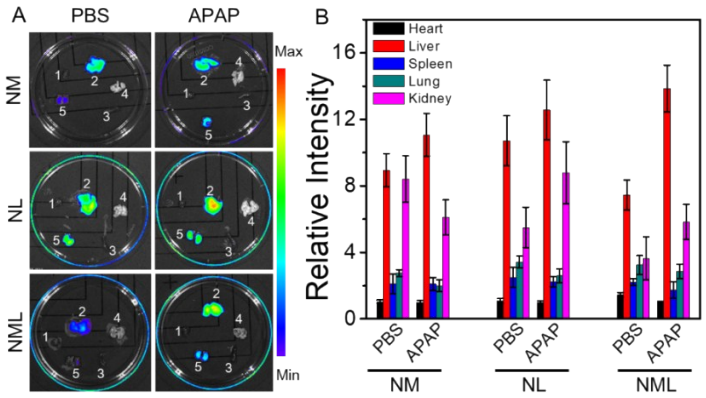

Fig. S18 (A) Fluorescence images of representative organs of mice after intravenously injected with **NM**, **NL** and **NML** (50 μL, 100 μM) for 120 min. 1, Heart; 2, Liver; 3, Spleen; 4, Lung; 5, Kidney. (B) The fluorescence intensity of each organ in (A), respectively. Ex= 640 nm. The emission band was at 695-770 nm. The results are the mean standard deviation of five separate measurements.

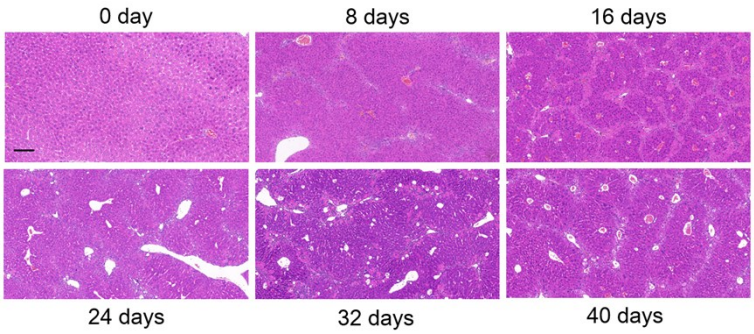

Fig. S19 Representative H&E staining images of the cirrhosis liver tissues in different days. Five mice were used to establish each group. Scale bar: 100 μm.

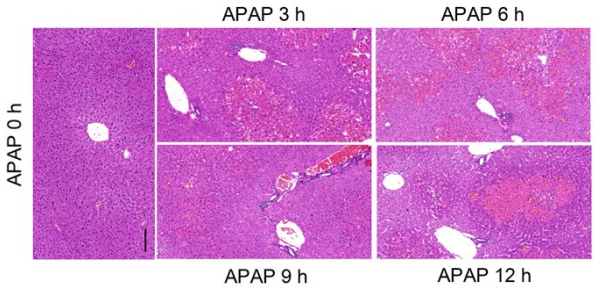

Fig. S20 Representative H&E staining images of APAP-induced liver injury for different times. Five mice were used to establish each group. Scale bar: 100 μm.

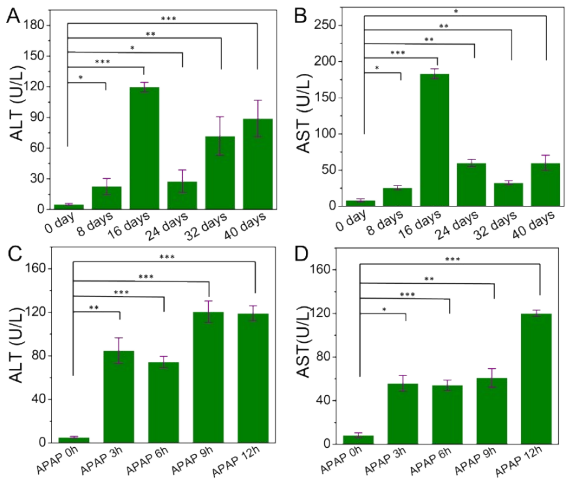

Fig. S21 (A) ALT and (B) AST level in serum of cirrhotic mice in different days. (C) ALT and (D) AST level in serum of APAP-induced liver injury mice in different times. The results are the mean standard deviation of five separate measurements. *$P < 0.05$, **$P < 0.01$, ***$P < 0.001$, compared with the control group (normal group).

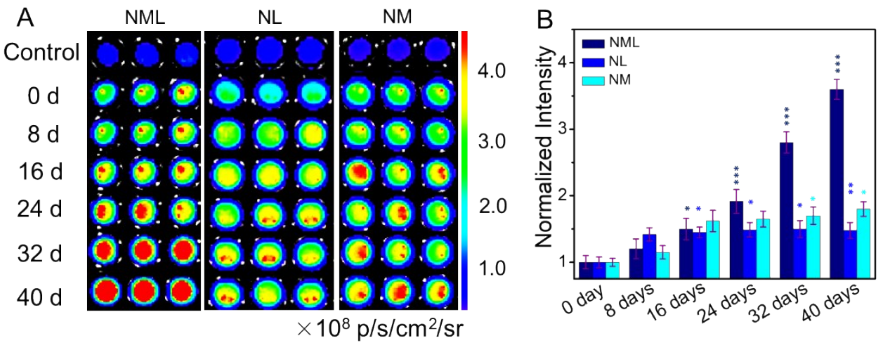

Fig. S22 (A) Fluorescence images of cirrhotic mouse serum samples in 96-well plates. The diluted serum samples (10 μL) were incubated with 20 μM **NML**, **NL** or **NM** in PBS solution for 2 h. Each row represents the representative parallel serum samples in the same mouse model. (B) Normalized fluorescence intensity of every ostiole for different administration days of cirrhotic mice in (A). The results are the mean standard deviation of five separate measurements. Ex= 640 nm. The emission band was at 695-770 nm. *$P < 0.05$, **$P < 0.01$, ***$P < 0.001$, compared with the control group (normal group).

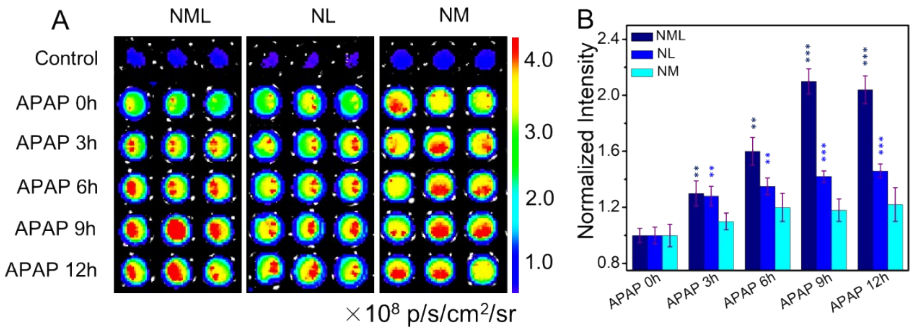

Fig. S23 (A) Fluorescence images of DILI serum samples in 96-well plates. The diluted serum samples (10 μL) were incubated with 20 μM **NML**, **NL** or **NM** in PBS solution for 2 h. Each row represents the representative parallel serum samples in the same mouse model. (B) Normalized fluorescence intensity of every ostiole for different administration times of DILI mice in (A). The results are the mean standard deviation of five separate measurements. Ex= 640 nm. The emission band was at 695-770 nm. **P* < 0.05, ***P* < 0.01, ****P* < 0.001, compared with the control group (normal group).

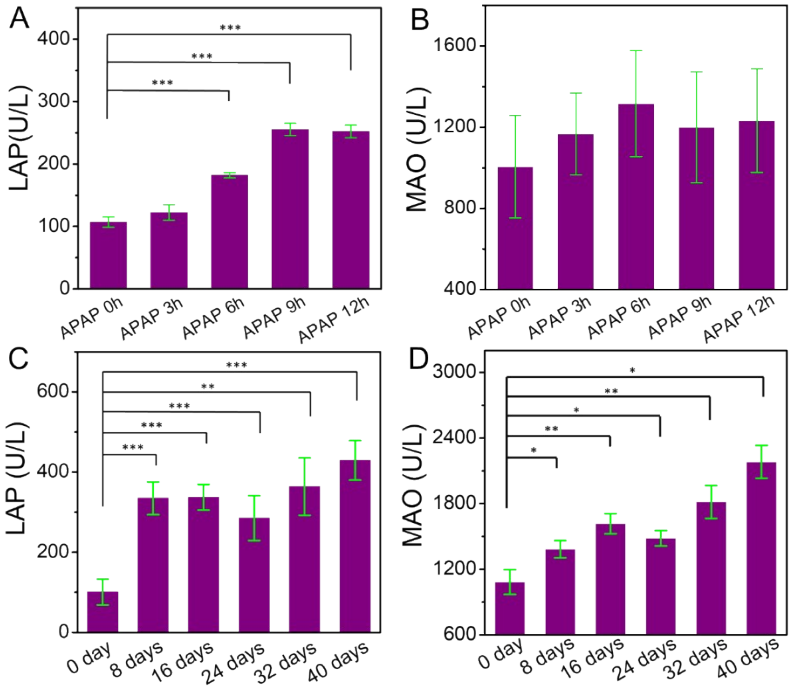

Fig. S24 (A) LAP and (B) MAO level in serum of APAP-induced liver injury mice in different times. (C) LAP and (D) MAO level in serum of cirrhotic mice in different days. The results are the mean standard deviation of five separate measurements. **P* < 0.05, ***P* < 0.01, ****P* < 0.001, compared with the control group (normal group).

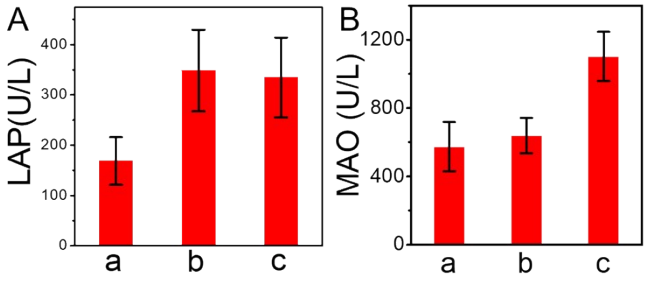

Fig. S25 (A) LAP and (B) MAO level in serum of human patients suffered from different hepatopathy. a: normal, b: hepatitis B patients, c: cirrhotic patients. The results are the mean standard deviation of three separate measurements.

4. MS and NMR spectra

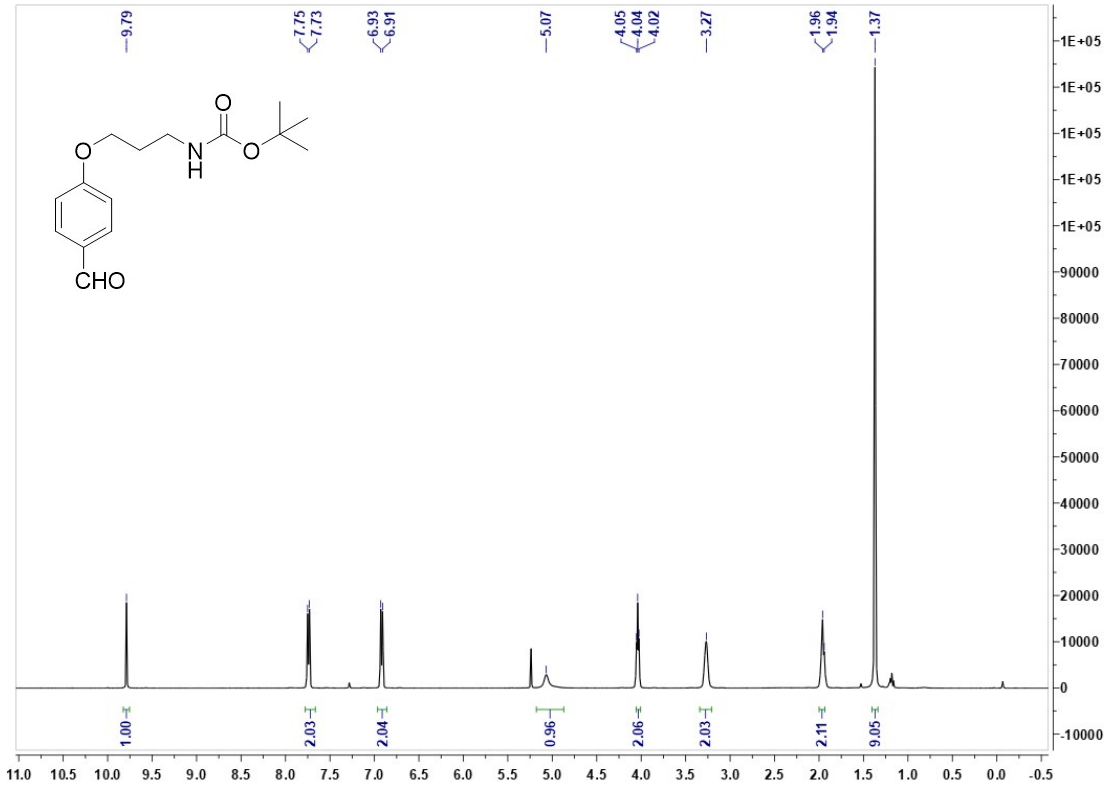

Fig. S26 ^{1}H NMR spectrum of compound 1.

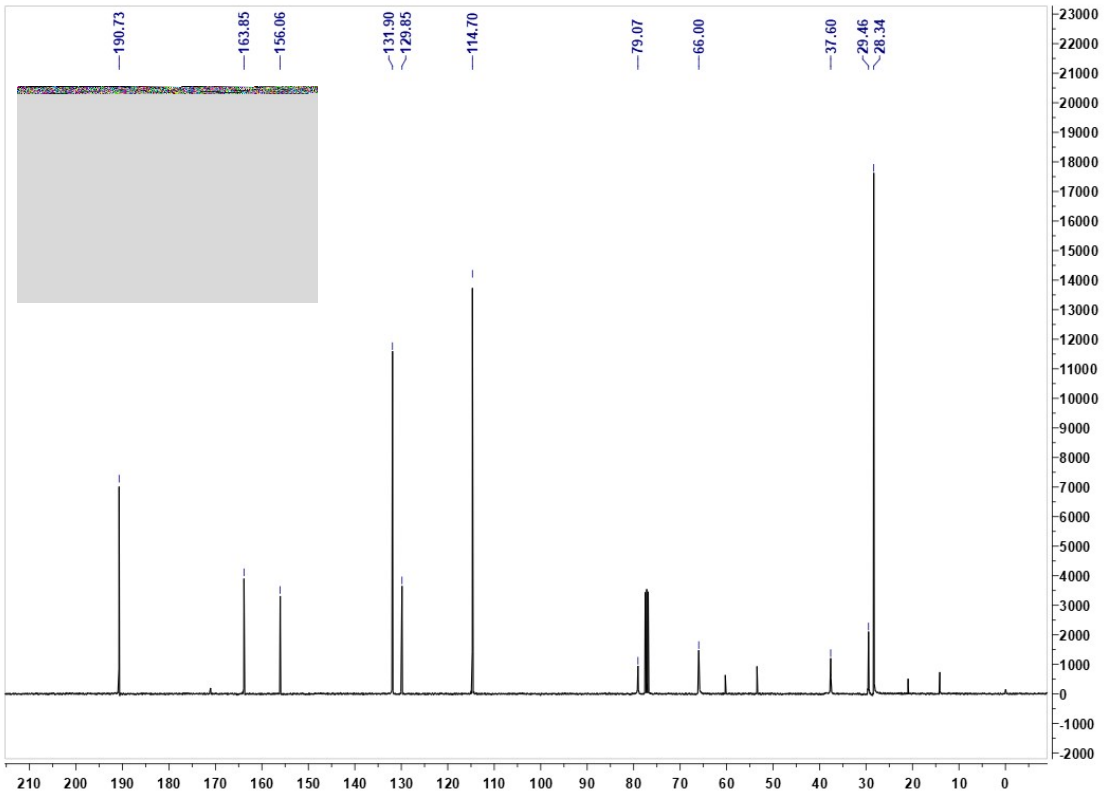

Fig. S27 ^{13}C NMR spectrum of compound 1.

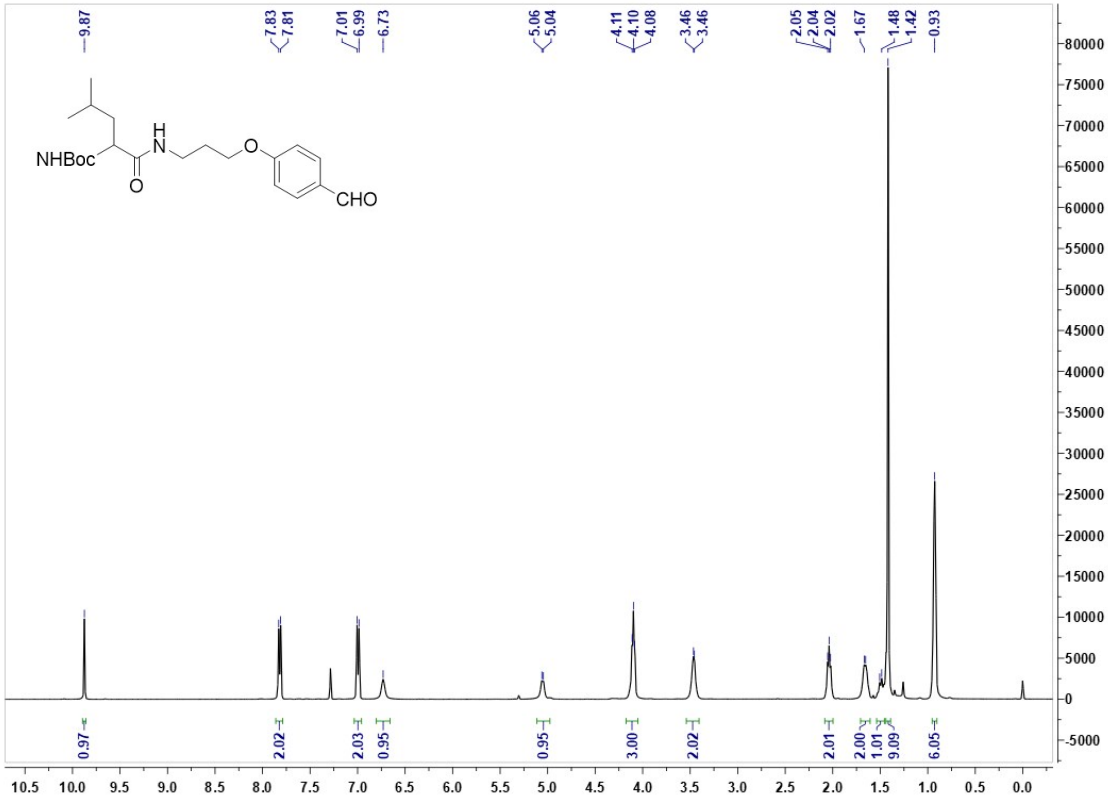

Fig. S28 ^{1}H NMR spectrum of compound 2.

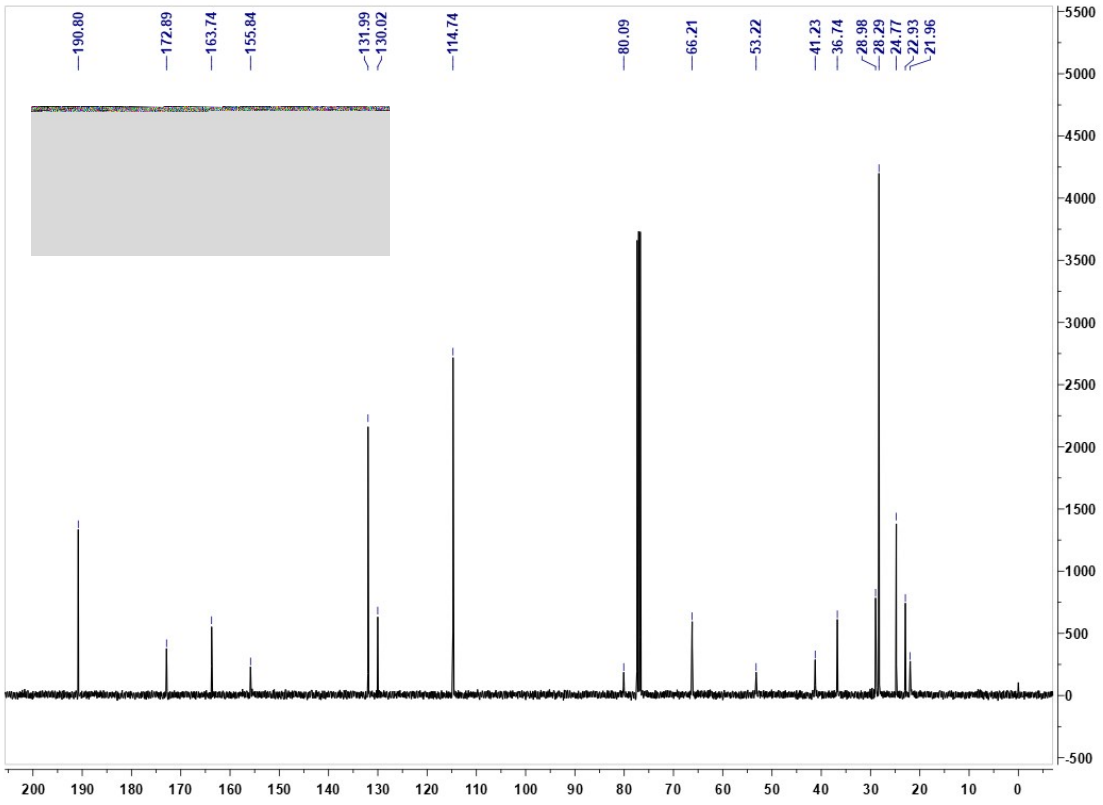

Fig. S29 ^{13}C NMR spectrum of compound 2.

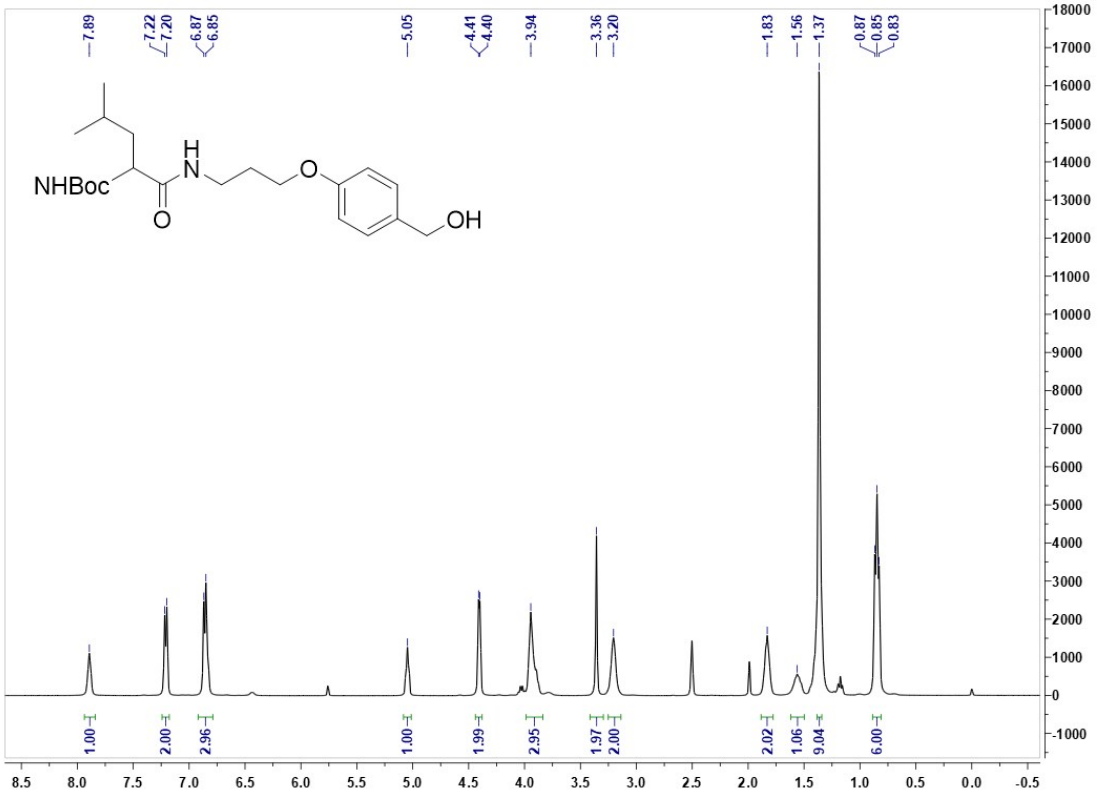

Fig. S30 ^{1}H NMR spectrum of compound 4.

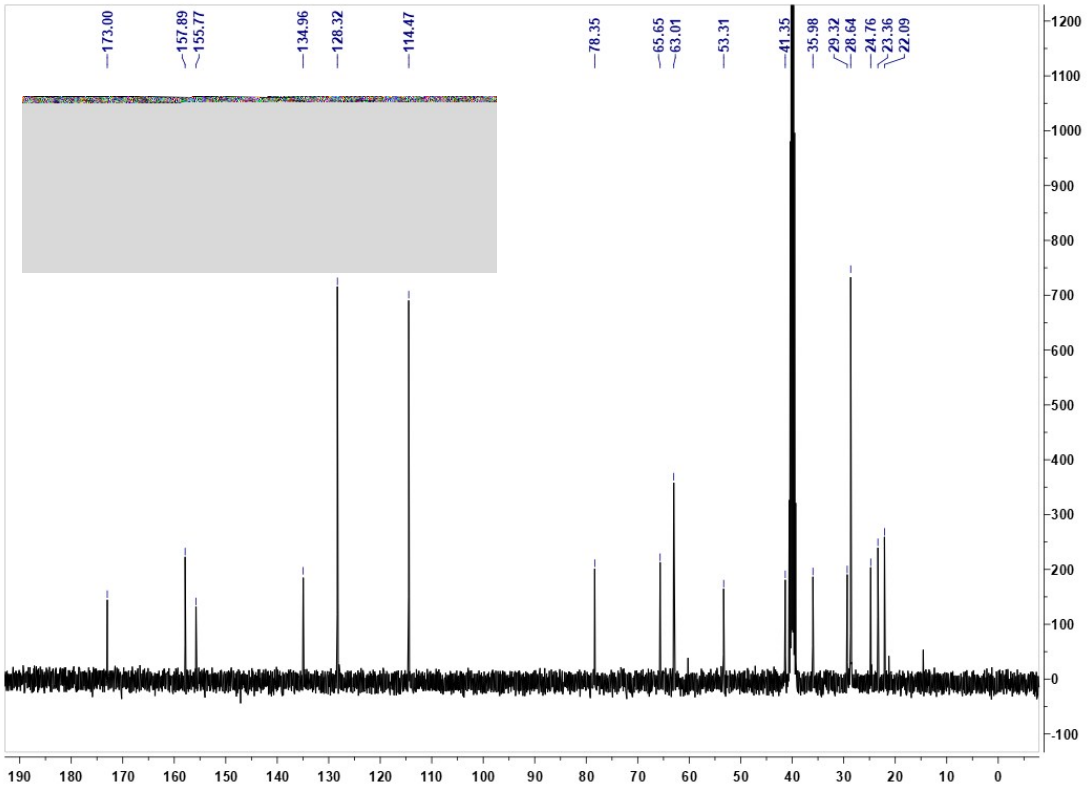

Fig. S31 ^{13}C NMR spectrum of compound 4.

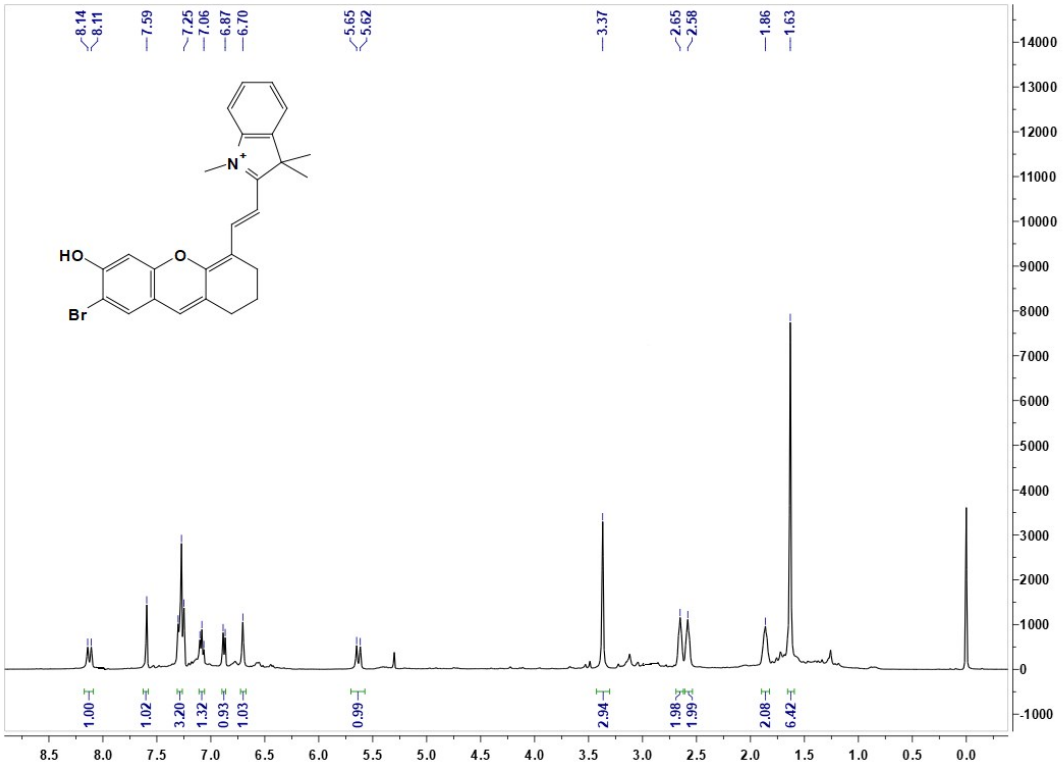

Fig. S32 ^{1}H NMR spectrum of compound 6.

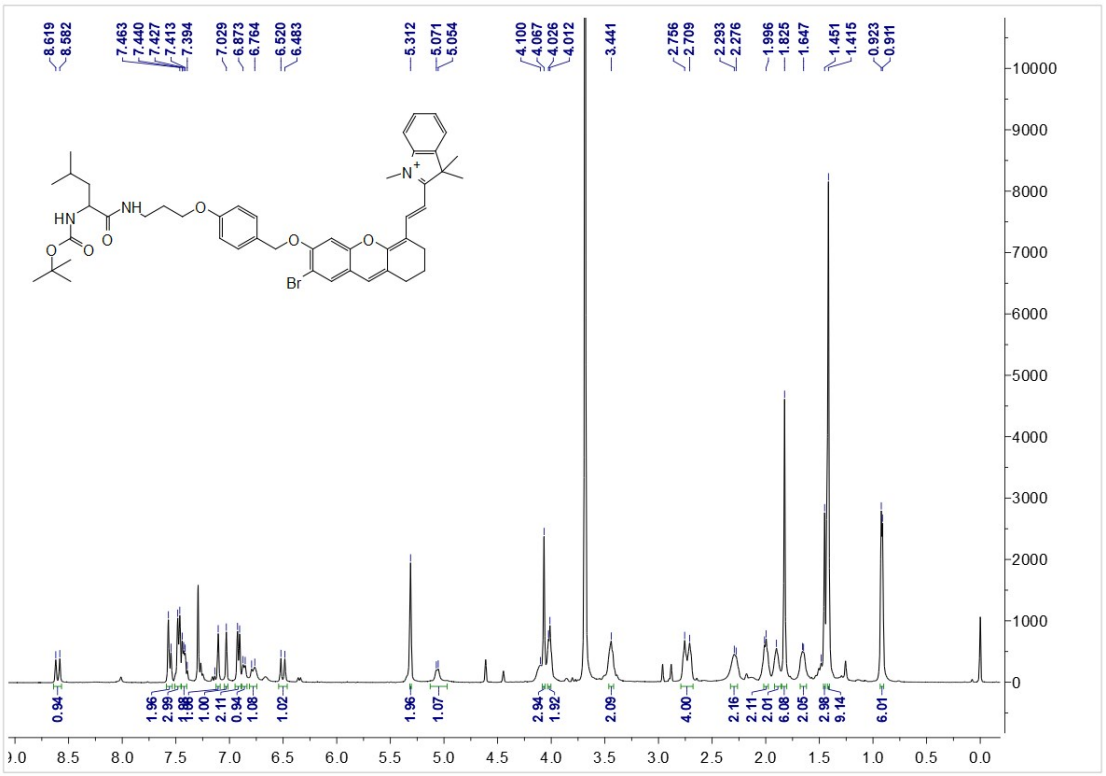

Fig. S33 ^{1}H NMR spectrum of compound 7.

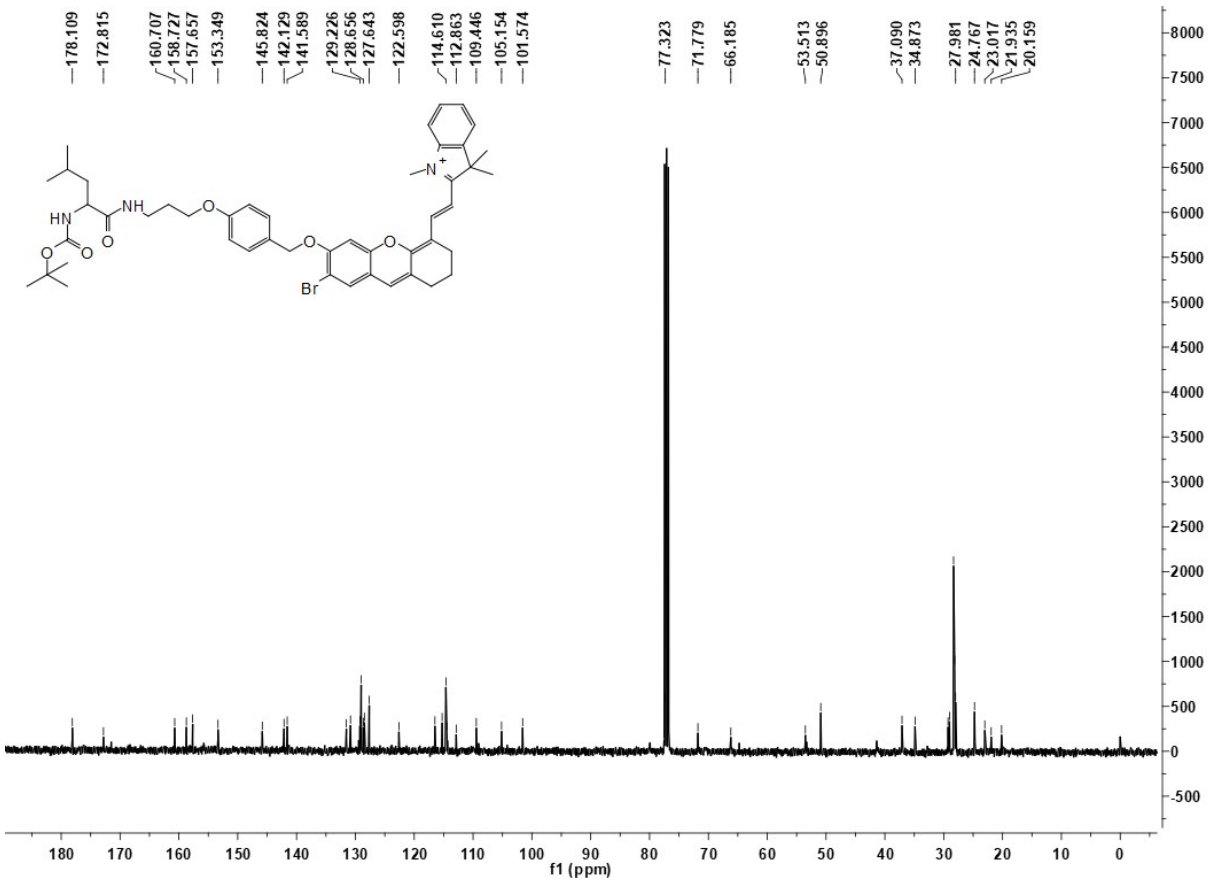

Fig. S34 ^{13}C NMR spectrum of compound 7.

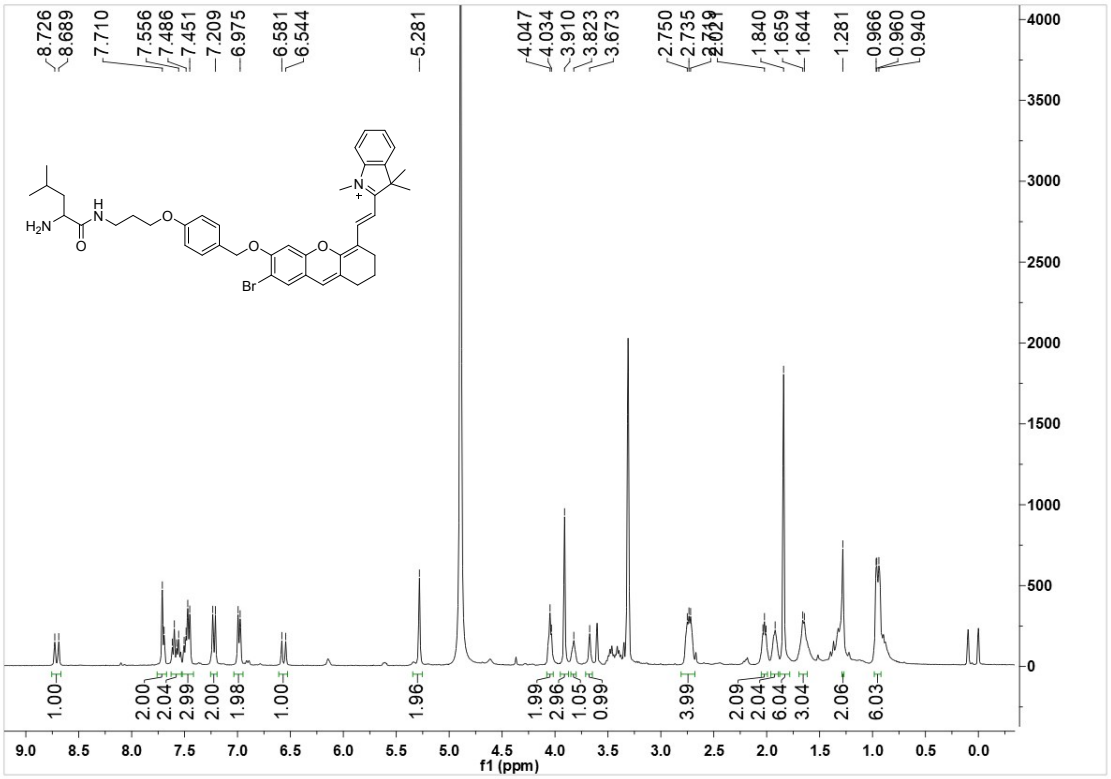

Fig. S35 [1]H NMR spectrum of **NML**.

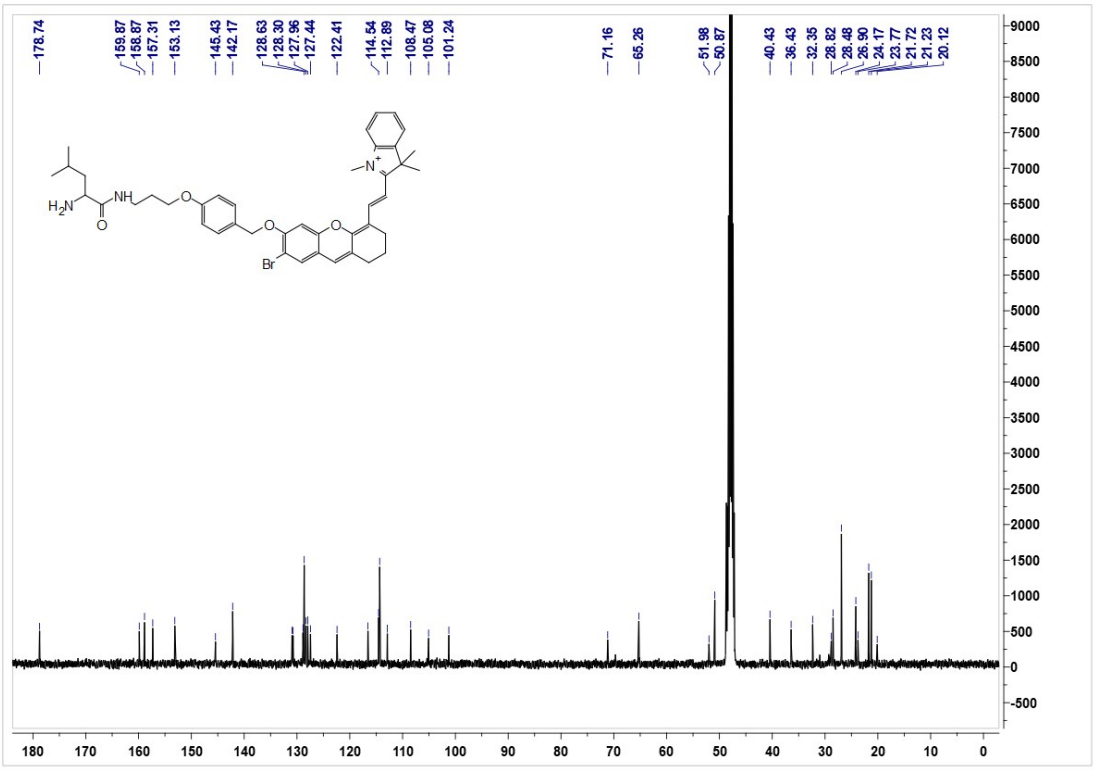

Fig. S36 [13]C NMR spectrum of **NML**.

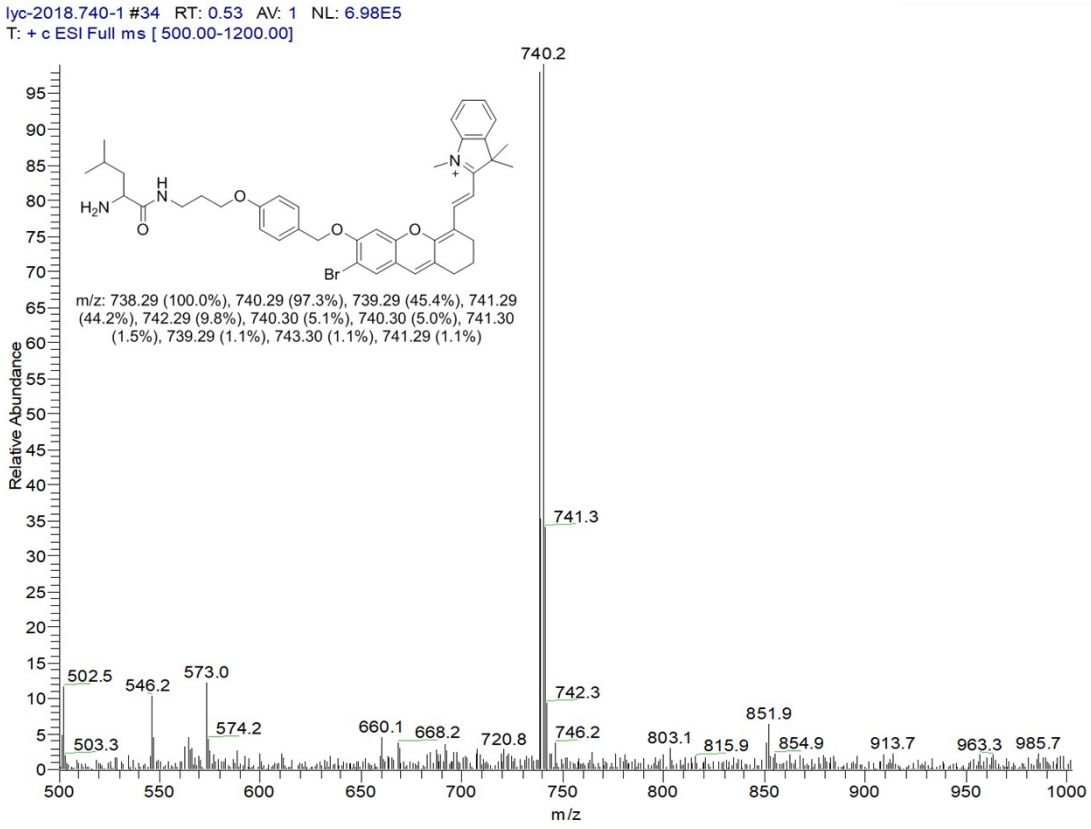

Fig. S37 ESI-MS spectrum of **NML**.

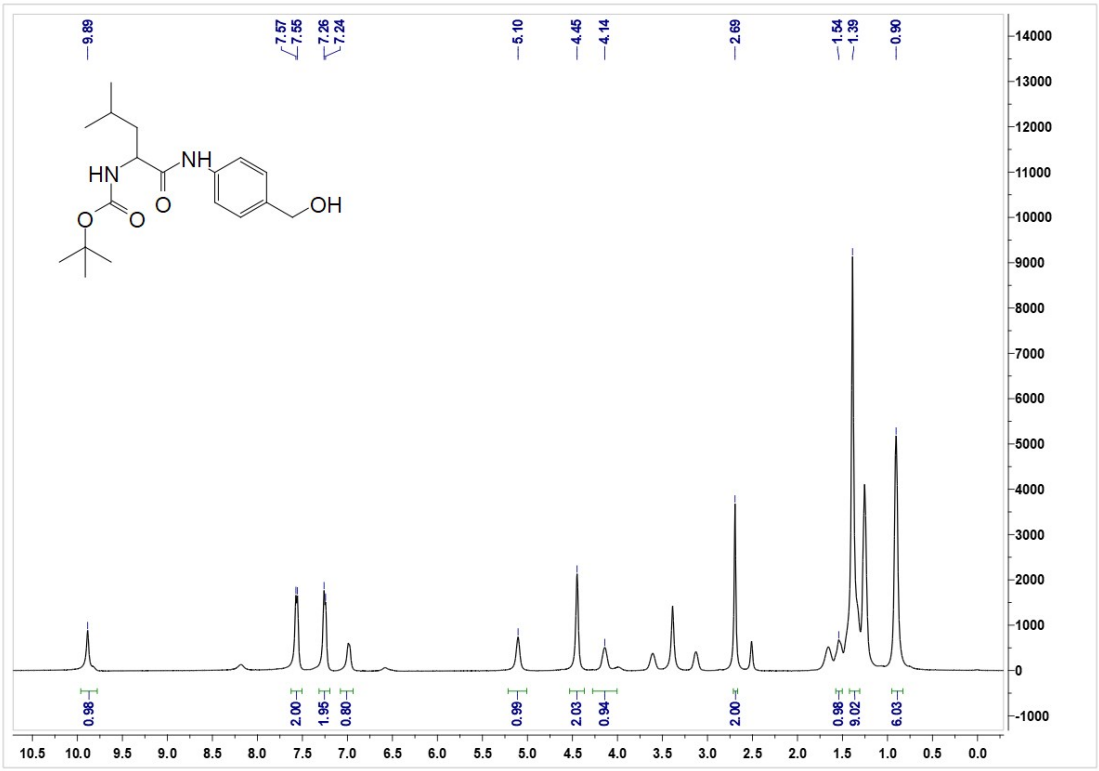

Fig. S38 ^{1}H NMR spectrum of compound 8.

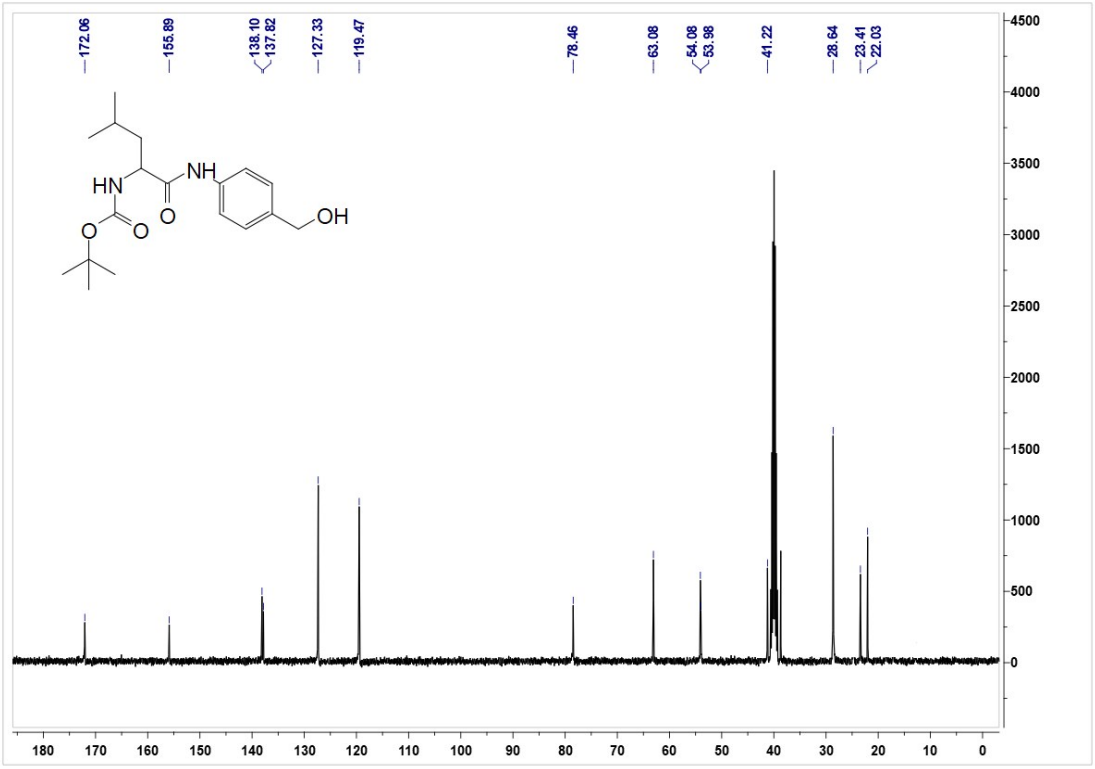

Fig. S39 ^{13}C NMR spectrum of compound 8.

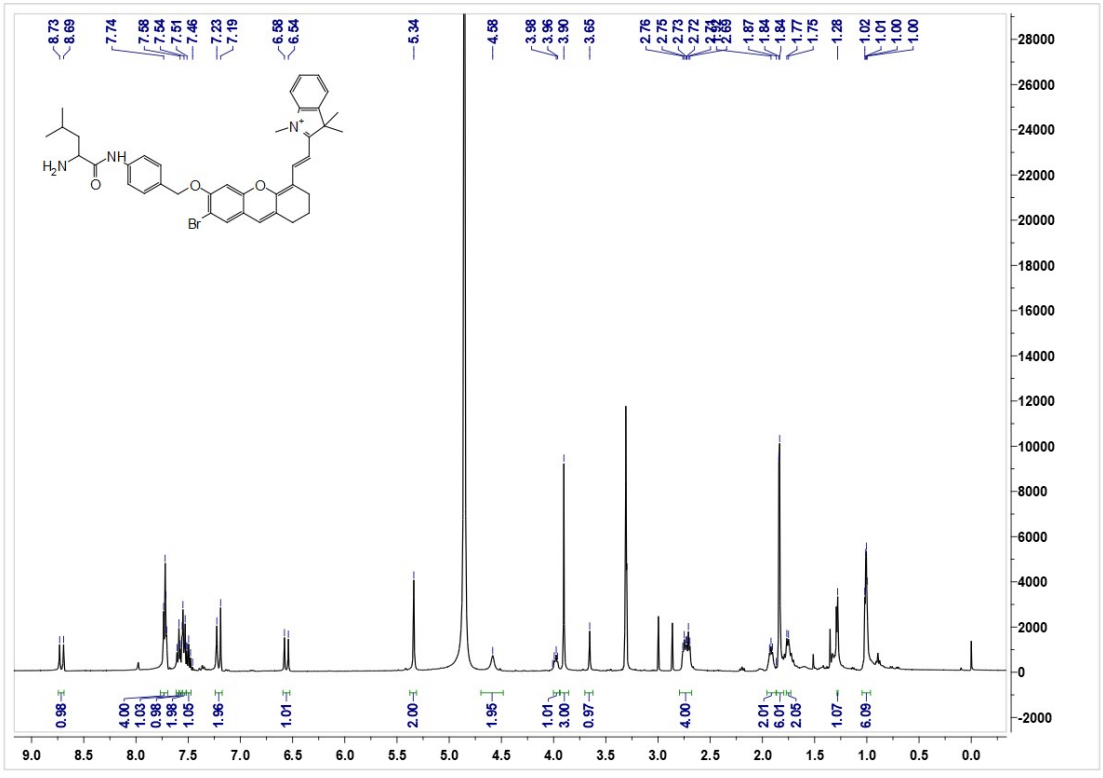

Fig. S40 ^{1}H NMR spectrum of **NL**.

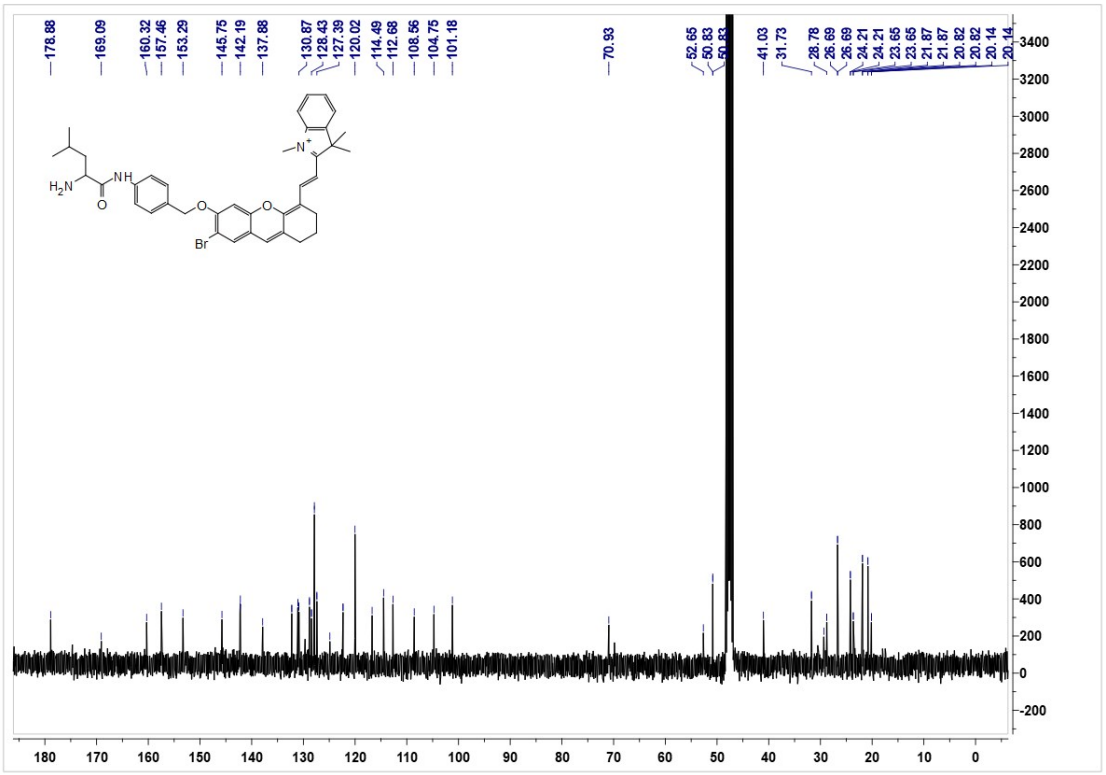

Fig. S41 ^{13}C NMR spectrum of **NL**.

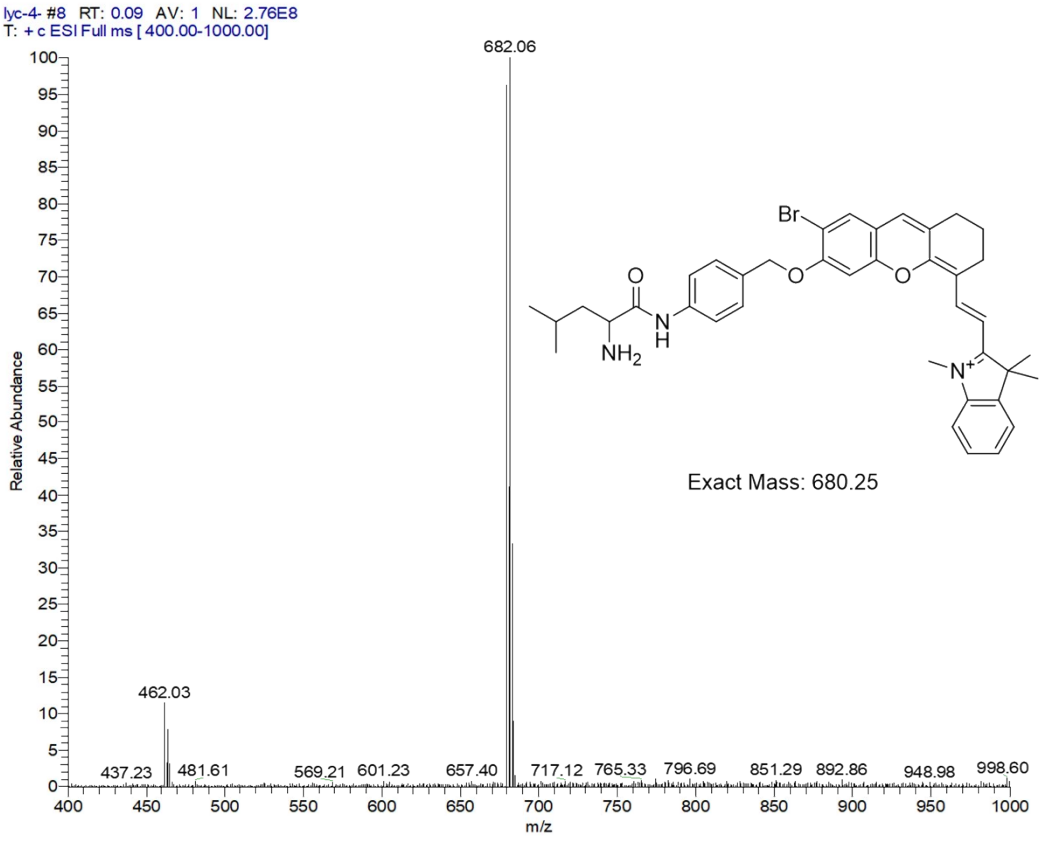

Fig. S42 ESI-MS spectrum of **NL**.

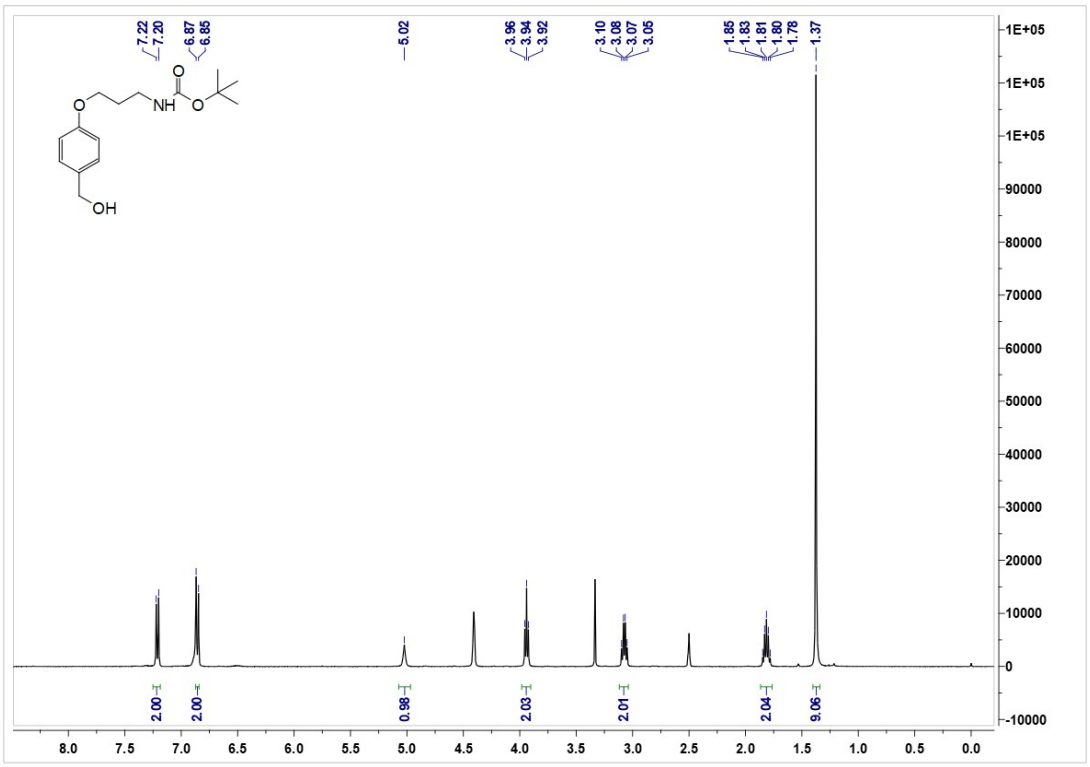

Fig. S43 ^{1}H NMR spectrum of compound 11.

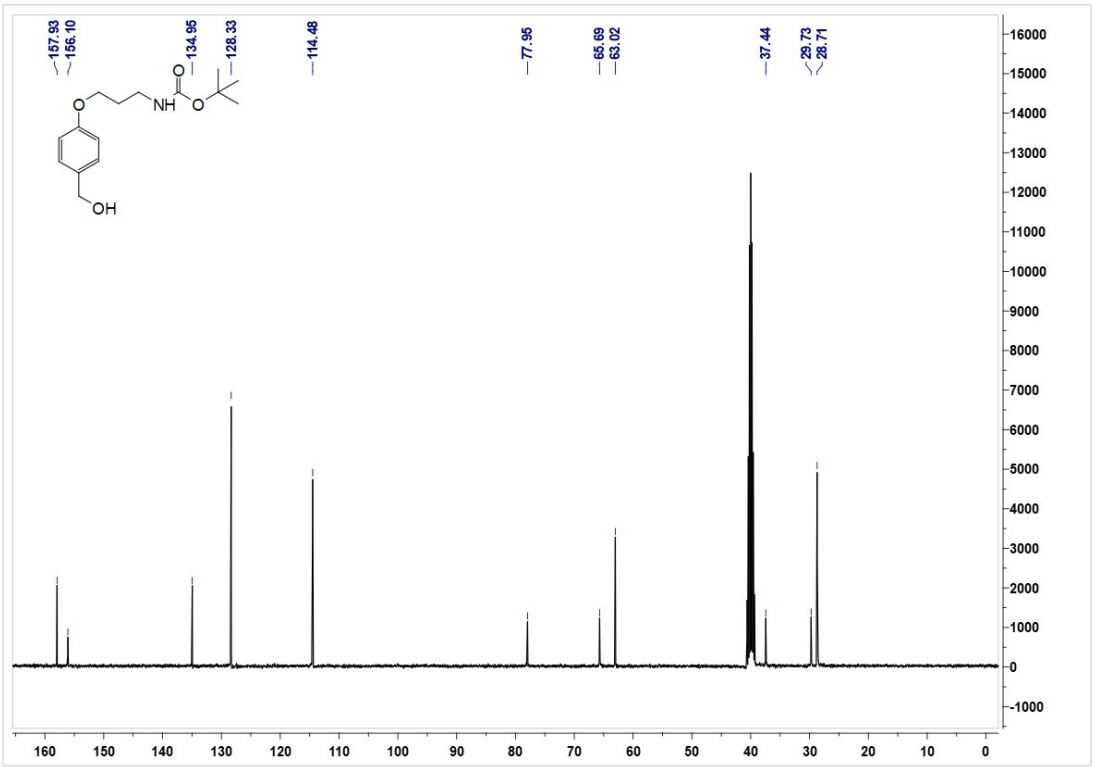

Fig. S44 ^{13}C NMR spectrum of compound 11.

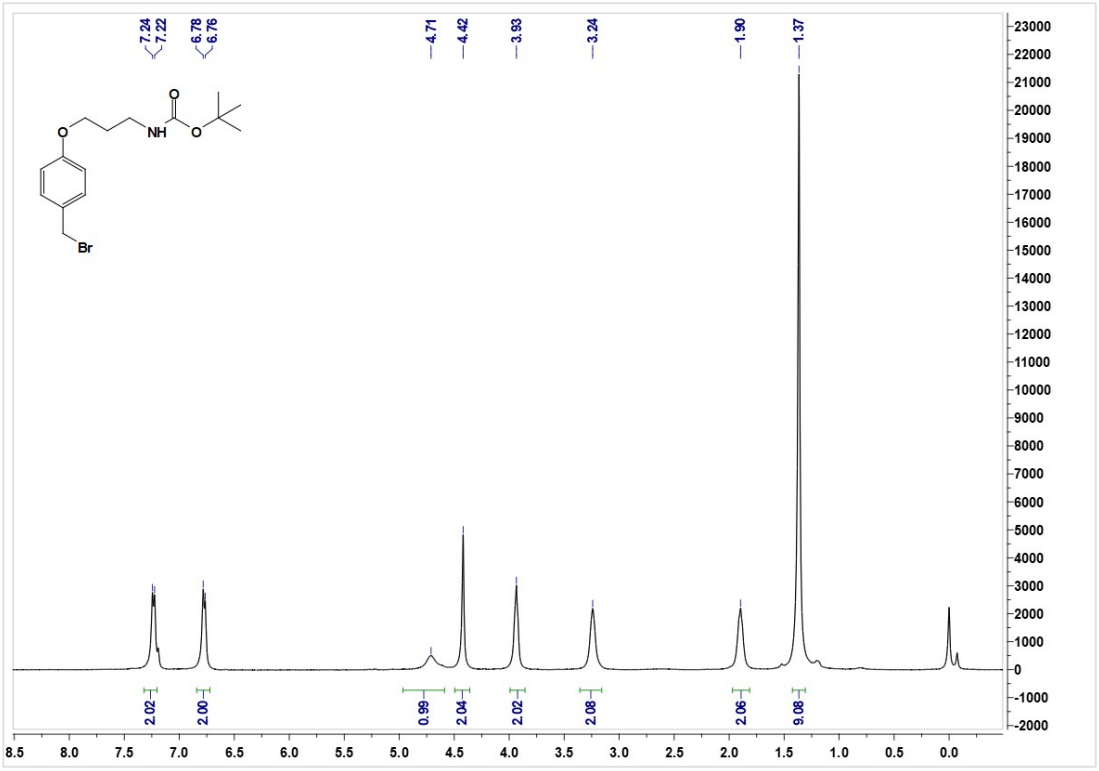

Fig. S45 ^{1}H NMR spectrum of compound 12.

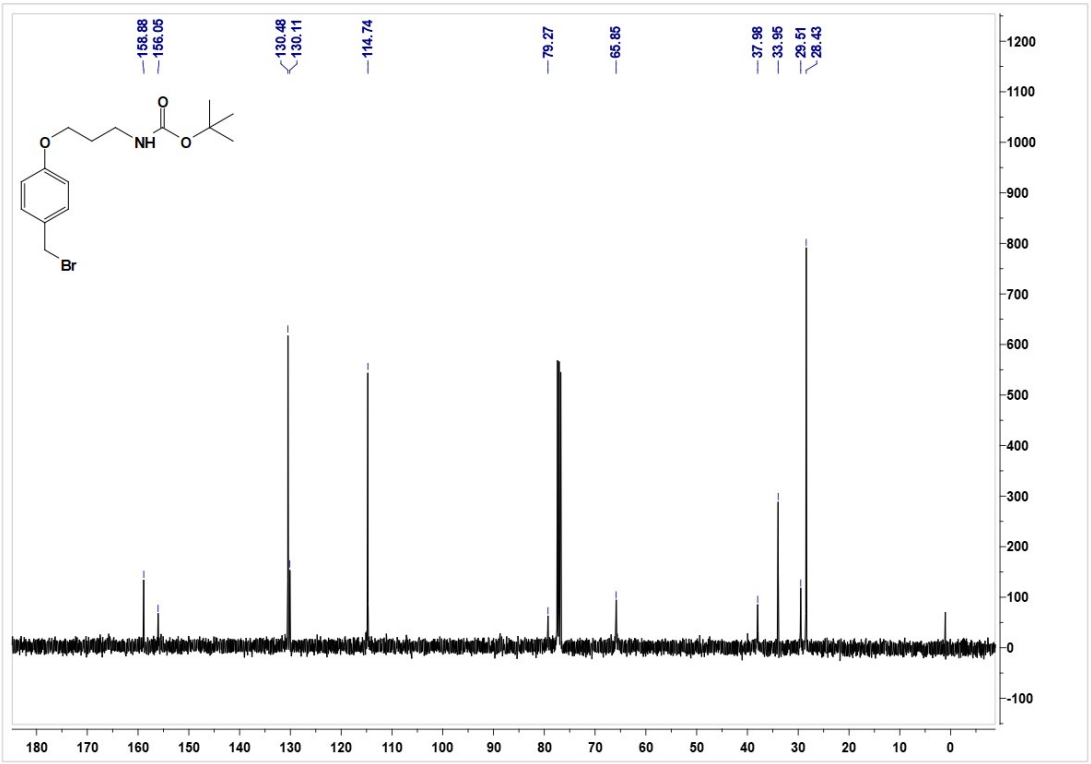

Fig. S46 ^{13}C NMR spectrum of compound 12.

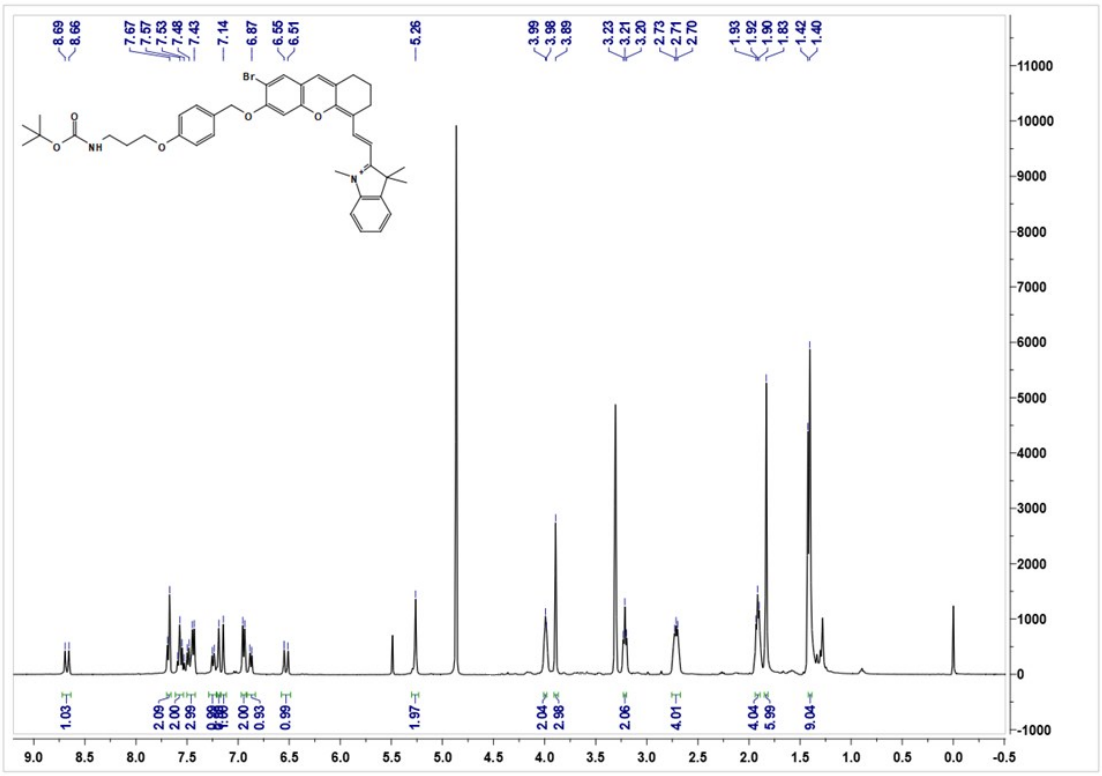

Fig. S47 ^{1}H NMR spectrum of compound 13.

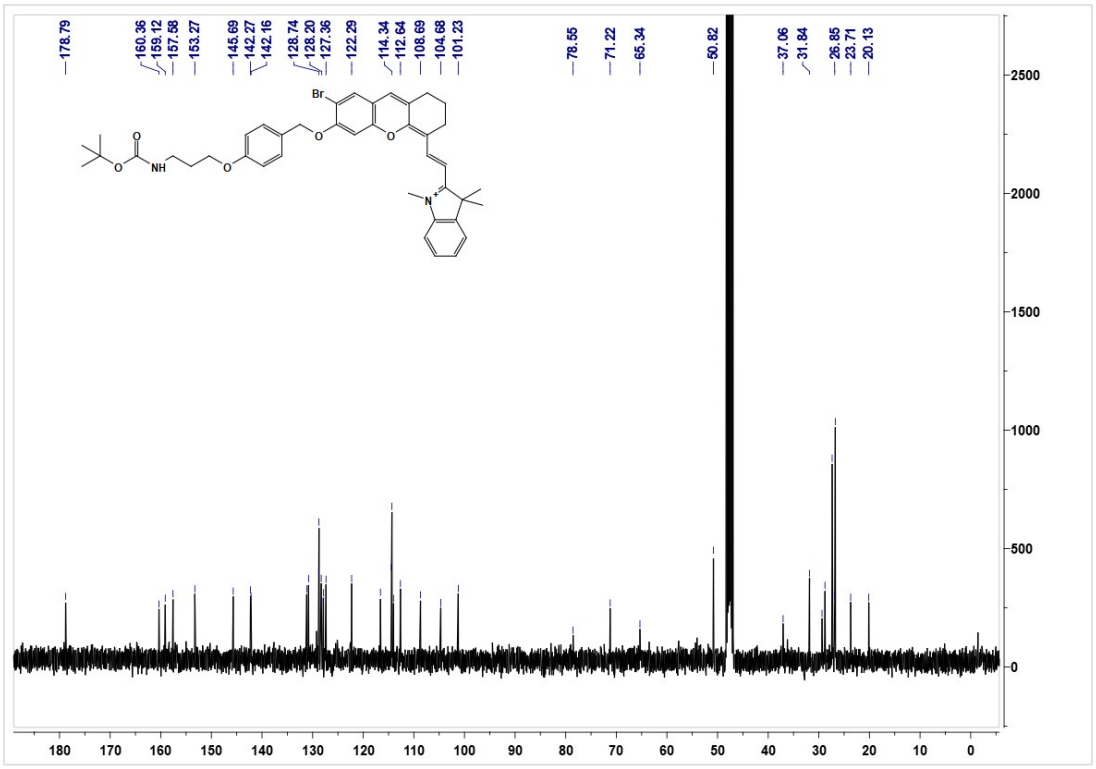

Fig. S48 ^{13}C NMR spectrum of compound 13.

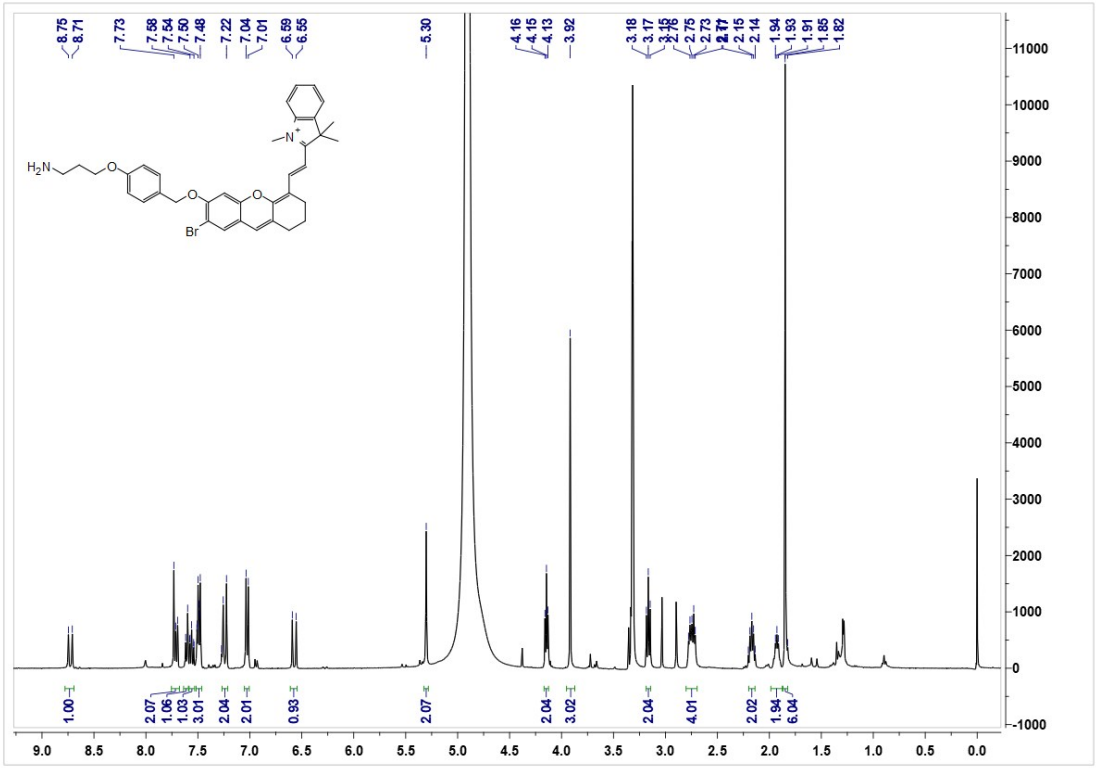

Fig. S49 ^{1}H NMR spectrum of **NM**.

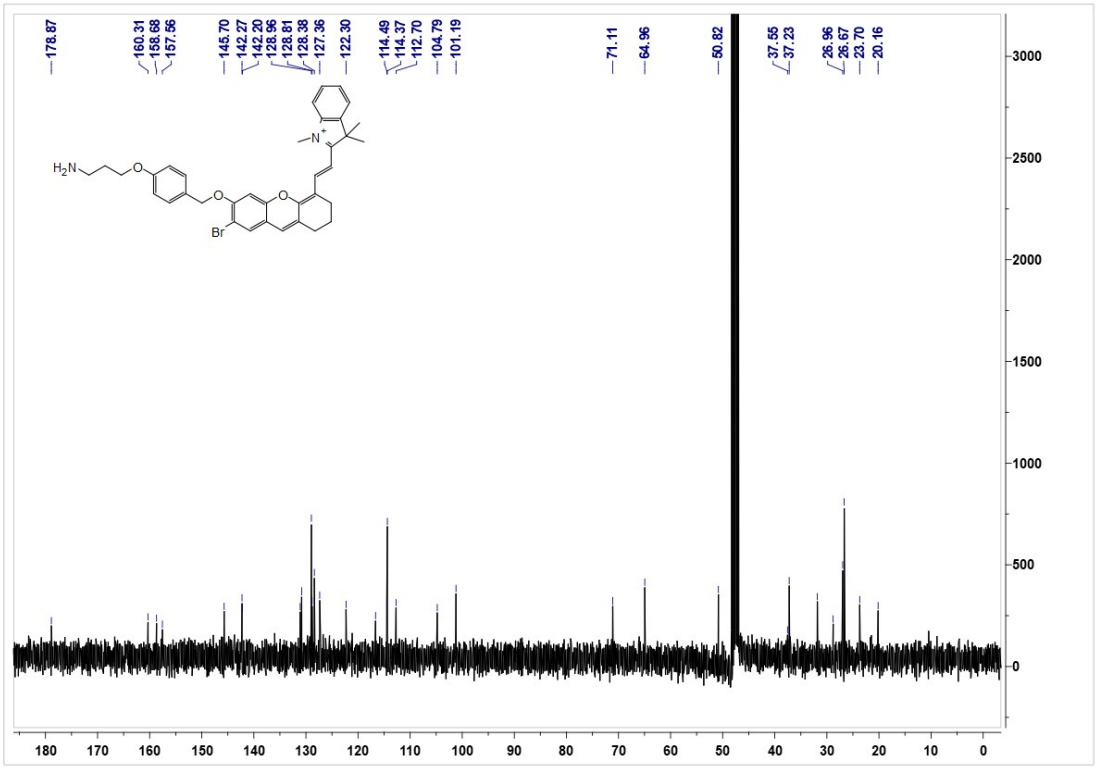

Fig. S50 ^{13}C NMR spectrum of **NM**.

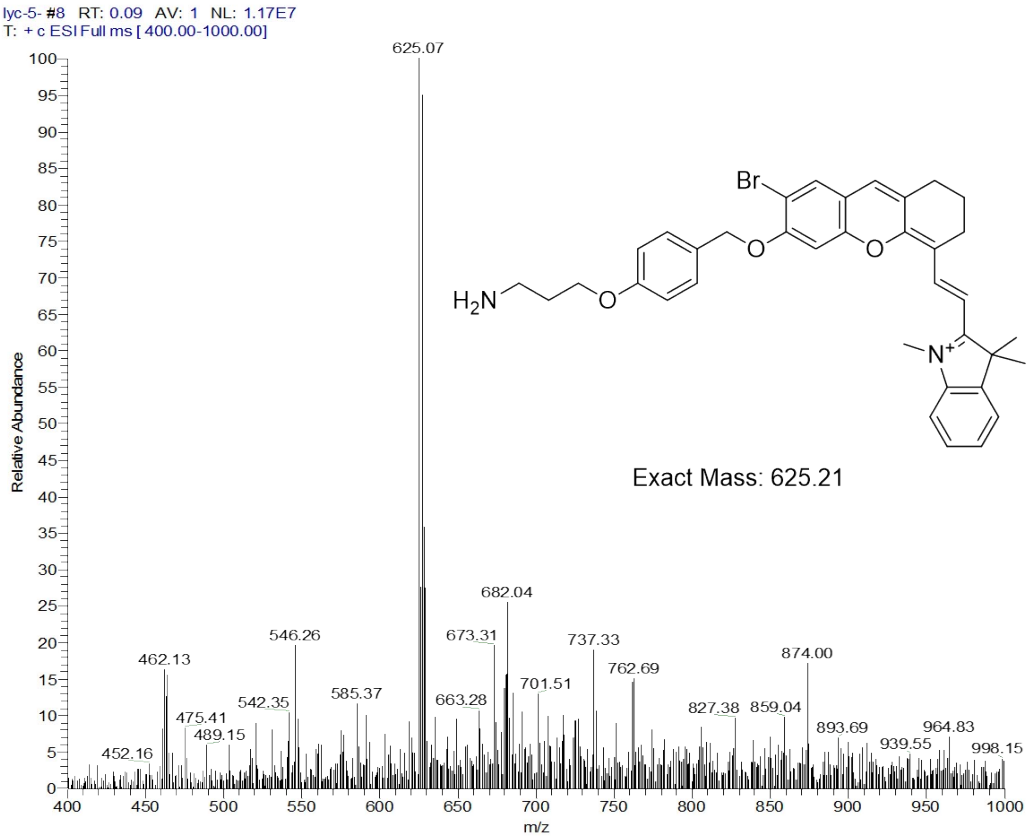

Fig. S51 ESI-MS spectrum of **NM**.